Cerebral Cortex March 2014;24:754–772
doi:10.1093/cercor/bhs356
Advance Access publication November 23, 2012

Scratch2 Modulates Neurogenesis and Cell Migration Through Antagonism of bHLH Proteins in the Developing Neocortex

Vanessa Paul[1,2], Anton B. Tonchev[1,3], Kristine A. Henningfeld[2,4], Evangelos Pavlakis[1], Barbara Rust[4], Tomas Pieler[2,4] and Anastassia Stoykova[1,2]

[1]Research Group Molecular Developmental Neurobiology, Max-Planck Institute for Biophysical Chemistry, 37077 Göttingen, Germany, [2]Cluster of Excellence "Nanoscale Microscopy and Molecular Physiology of the Brain (CNMPB)", Göttingen, Germany, [3]Department of Anatomy, Histology and Embryology, Medical University, 9002 Varna, Bulgaria and [4]Department of Developmental Biochemistry, University of Göttingen, 37077 Göttingen, Germany

Address correspondence to Anastassia Stoykova, Research Group Molecular Developmental Neurobiology, Max Planck Institute for Biophysical Chemistry, Am Fassberg 11, 37077 Goettingen, Germany. Email: astoyko@gwdg.de

Scratch **genes (*Scrt*) are neural-specific zinc-finger transcription factors (TFs) with an unknown function in the developing brain. Here, we show that, in addition to the reported expression of mammalian *Scrt2* in postmitotic differentiating and mature neurons in the developing and early postnatal brain, Scrt2 is also localized in subsets of mitotic and neurogenic radial glial (RGP) and intermediate (IP) progenitors, as well as in their descendants—postmitotic IPs and differentiating neurons at the border subventricular/intermediate zone. Conditional activation of transgenic *Scrt2* in cortical progenitors in mice promotes neuronal differentiation by favoring the direct mode of neurogenesis of RGPs at the onset of neurogenesis, at the expense of IP generation. Neuronal amplification via indirect IP neurogenesis is thereby extenuated, leading to a mild postnatal reduction of cortical thickness. Forced in vivo overexpression of *Scrt2* suppressed the generation of IPs from RGPs and caused a delay in the radial migration of upper layer neurons toward the cortical plate. Mechanistically, our results indicate that Scrt2 negatively regulates the transcriptional activation of the basic helix loop helix TFs Ngn2/NeuroD1 on E-box containing common target genes, including *Rnd2*, a well-known major effector for migrational defects in developing cortex. Altogether, these findings reveal a modulatory role of Scrt2 protein in cortical neurogenesis and neuronal migration.**

Keywords: cortex, migration, neurogenesis, Scratch2

Introduction

The cerebral cortex (pallium) is the most complex structure of the brain composed of an astonishing diversity of neuronal and glial cells. The glutamatergic neurons of the neocortex (located in the dorsal pallium) are arranged in 6 layers, and numerous functional domains that send axonal projections to intracortical, subcortical, and subcerebral targets. The vast majority of the neocortical neurons are generated during development by radial glial progenitors (RGPs) and their descendants, the intermediate progenitors (IPs), located in the cortical ventricular (VZ) and subventricular zone (SVZ), respectively (reviewed by Götz and Huttner 2005). Compelling recent evidence indicates that area identity is specified in VZ progenitors through combinatorial expression of transcription factors (TFs), cell adhesion molecules, and axon-guiding molecules and ligands (Rakic 1988; Sur and Rubenstein 2005; Mallamaci and Stoykova 2006; Rash and Grove 2006; O'Leary and Sahara 2008; Borello and Pierani 2010). Neurons of the distinct radial layers are generated in a tightly controlled temporal order with a stereotypical "inside layers (L6, L5) first–outside layers (L4, L3, L2) last" pattern (Rakic 1974; McConnell 1991; Caviness and Takahashi 1995; Nowakowski et al. 2002). In each of these layers, the neurons exhibit a specific pattern of arrangement, molecular and functional properties (Hevner et al. 2003, 2006; Arlotta et al. 2005).

During corticogenesis, RGPs undergo different types of cell division at the apical surface of the VZ (Miyata et al. 2001; Anthony et al. 2004; Haubensak et al. 2004; Malatesta et al. 2003; 2008): 1) Symmetric division (self-renewal), giving rise to 2 RGP daughter cells; 2) asymmetric division, generating an RGP (self-renewal) and an neuron (direct mode of neurogenesis), and 3) asymmetric division, generating the RGP and an IP that accumulates in the SVZ (Götz and Huttner 2005; Pontious et al. 2008). Most of the IPs are exclusively neurogenic, directly generating 2 neuronal daughter cells (indirect mode of neurogenesis). However, a small fraction of IPs undergoes up to 3 rounds of proliferation and subsequently give rise to neurons (Haubensak et al. 2004; Miyata et al. 2004; Noctor et al. 2004; Wu et al. 2005), thereby amplifying the output of distinct neuronal fates generated at a given developmental stage (Noctor et al. 2004; Arnold et al. 2008; Pontious et al. 2008). While the indirect mode of neurogenesis is most prominent at mid-corticogenesis (with a peak in mouse at E14.5), the direct mode of neurogenesis seems to predominate at early stages (E10–E13 in mouse). Recent evidence indicates, however, that IPs also exist in the VZ during early neurogenesis, suggesting that IPs may contribute to the generation of both early- and late-born neurons with low (LL) and upper layer (UL) identities (Haubensak et al. 2004; Englund et al. 2005; Kowalczyk et al. 2009). In contrast to RGPs, the IPs express neither the TF Pax6, shown to be an intrinsic determinant of the neurogenic ability of RGPs (Götz et al. 1998; Heins et al. 2002) nor members of the pro-proliferative Hes family of TFs (Ohtsuka et al. 2001; Englund et al. 2005; Cappello et al. 2006). IPs, on the other hand, are distinguished by the specific expression of TFs Eomes/Tbr2 (Englund et al. 2005), Cux1 and Cux2 (Nieto et al. 2004; Zimmer et al. 2004; Cubelos et al. 2008), Ngn2 (Miyata et al. 2004), Svet1 (Tarabykin et al. 2001), and as recently shown, Insulinoma −1 (Insm1; Farkas et al. 2008).

We identified the mammalian *Scratch2* (*Scrt2*) in a microarray screen as a gene with regionalized expression in the SVZ/IZ of the caudomedial pallium (Mühlfriedel et al. 2007). The *Scratch* genes constitute an independent subgroup of the *Snail* superfamily of TFs generated during evolution through a duplication of a single *Snail* gene in the metazoan ancestor (Nieto 2002; Barrallo-Gimeno and Nieto 2009). In vertebrates,

2 *Snail* and 2 *Scratch* genes (*Scrt1* and *Scrt2*) have been identified. Members of the *Snail/Scratch* superfamilies are characterized by a conserved C-terminus, containing 4–6 zinc fingers (ZFs) of the C_2H_2 (cysteine/histidine) type, which mediate DNA-binding to CANNTC E-box motifs that are also core-binding sites of the neurogenic basic helix loop helix (bHLH) transcription factors (TFs) (Barrallo-Gimeno and Nieto 2009). The N-terminus of the vertebrate Snail/Scratch proteins contains a more divergent SNAG domain that has been shown to be necessary for the transcriptional repression and nuclear localization activities of the rat Gfi oncoprotein (Grimes et al. 1996). However, this function does not seem to be conserved in the human *SCRT1* (Nakakura et al. 2001). The *Scratch* genes are expressed exclusively in the nervous system of all species analyzed to date (Roark et al. 1995; Nakakura et al. 2001; Marin and Nieto 2006). While *Scrt1* orthologs in *Drosophia* (Roark et al. 1995), *Caenorhabditis elegans* (*ces-1*; Metzstein and Horvitz 1999), zebrafish (Dam et al. 2011), and human (*SCRT1*; Nakakura et al. 2001; Nakakura et al. 2001) have been shown to promote neuronal differentiation and survival, the function of mammalian *Scratch2* is unknown.

Here, we have assessed Scrt2 function in the developing mouse cortex by conditional activation of *Scrt2* in the developing dorsal pallium of transgenic mice and clonal cell-pair analyses in cortical cultures after forced Scrt2 expression via in utero electroporation (IUE). Our results revealed that Scrt2 acts as a modulator of neuronal differentiation and migration in the developing mammalian cortex.

Materials and Methods

Animals

Animals were handled in accordance with the German Animal Protection Law. The applied strategy to generate the mouse (*Mus musculus*) line (named *JoScrt2*) allowing in vivo overexpression of the murine *Scrt2* is depicted in Supplementary Figure 2*A*. Proven founders were crossed with *Emx1-Cre* line (Gorski et al. 2002) and genotyped by fluorescence microscopy for GFP and genotyping polymerase chain reactions (PCRs) for *Cre* and *β-galactosidase* genes. *JoScrt2* and *Emx1-Cre* mice were maintained in a C57BL6N background. CD1 mice were used for in utero experiments and clonal pair-cell analyses.

Generation of Transgenic Mice for In Vivo Overexpression of Scrt2

For conditional activation of *Scrt2*, the construct *pJoScrt2* was generated. Synthetically generated, codon-optimized cDNA, coding for the Scrt2 (GenScript; sequence shown in Supplementary Fig. 1*C*) was inserted into the *XhoI* site of pJoJo vector (Berger et al. 2007) downstream of a cytomegalovirus (CMV)/β-actin promoter followed by *internal ribosome entry site-lacZ*-reporter sequence (Supplementary Fig. 2*A*). To ensure a correct recombination in culture, the plasmid was used to generate *JoScrt2* mice by pronuclear microinjection, and positive *JoScrt2* founder mice were identified by GFP fluorescence. After crossing with female mice from the *Emx1-Cre* line, the double transgenic mice (*JoScrt2*; *Emx1Cre*) display a specific loss of GFP fluorescence in the dorsal telencephalon and allow the CMV/β-actin promoter to drive the expression of *Scrt2* together with the l*acZ*-reporter. Double transgenic animals were identified by genomic PCR with primers (5′ → 3′) for GFP (F: accctgaagttcatctggacc; R: tgggtgctcaggtagtggttg), lacZ (F: cgtcacactacgtctgaacgtcg; R: cagacgattcattggcaccatgc), and Cre (F: atgcttctgtccgtttgccg; R: cctgttttgcacgttcaccg). In total, 2 transgenic lines were generated, both showing similar same capacity.

In Situ Hybridization and X-gal Staining

In Situ Hybridization (ISH) using digoxigenin (DIG)-labeled riboprobes (double ISH with fluorescein-labeled riboprobes) was performed on 16-µm cryostat sections as described previously (Mühlfriedel et al. 2007). EST (GenBank Accession No. AK090280) was used to generate murine *Scrt2* in situ probe with a length of 664 bp. For detection of β-galactosidase enzymatic activity, embryonic brains were fixed and stained (2–12 h, depending on the stage for isolation) at 30°C with X-gal substrate (Invitrogen).

Immunohistochemistry

For immunohistochemistry (IHC), 8–16 µm cryosections (from fixed in 4% paraformaldehyde/phosphate buffer saline (PFA/PBS) and cryoprotected in 20% sucrose brains) were blocked with normal sera of the appropriate species and incubated overnight with primary antibody. The following primary antibodies were used: rat anti-bromodeoxyuridine (anti-BrdU) (1:200 for BrdU and CidU, Abcam), mouse anti-BrdU (1:100 for BrdU and iododeoxyuridine (IdU), Becton Dickinson or Caltag), rabbit anti-caspase-3 (1:200; Cell Signalling), mouse anti-Cre (1:200; Sigma), rat anti-Ctip2 (1:200; Abcam), rabbit anti-Cux1 (1:250; Santa Cruz), chicken anti-GFP (1:500; Abcam), guinea pig anti-Insm1 (1:20.000, a gift from C. Birchmeier), mouse anti-Nestin (1:100; Millipore), mouse anti-NeuN (1:100; Chemicon), mouse anti-Neurofilament (1:100; Abcam), mouse anti-Ngn2 (1:10; a gift from D.J. Anderson), mouse anti-Ngn2 (1:50; R&D systems), rabbit anti-Pax6 (1:300; Covance), mouse anti-Pax6 (1:100; Developmental Studies Hybridoma Bank, DHSB), mouse anti-phospho-histone H3 (1:50; Cell Signalling), rabbit anti-Scrt2 (P-20/sc-85910; 1:50; Santa Cruz Biotech), rabbit anti-Scrt2 (1:50; Sigma-Aldrich, SAB2102096), rabbit anti-Tbr1 (1:300; Abcam), rabbit anti-Tbr2 (1:200; Chemicon), and mouse anti-βIII tubulin (1:400, Chemicon). Primary antibodies were detected with appropriate secondary antibodies conjugated to Alexa Fluor fluorophores (Invitrogen), and sections were counterstained with Vectashield mounting medium containing 4′,6′-diamidino-2-phenylindole (DAPI; Vector Laboratories) to label the cell nuclei. Whenever necessary, antigen retrieval was applied using the Vector Unmasking Solution (Lector Laboratories) in a microwave over (800 W) for 3 times of 5 min.

BrdU, CidU, and IdU Labeling

BrdU, CidU, and IdU were injected intaperitoneally. The following concentrations have been used; BrdU: 140 mg/kg of body weight, CidU: 50 mg/kg of body weight, and IdU: 50 mg/kg of body weight.

Western Blotting

Cortices from *Scrt2GOF* transgenic mice and wild-type littermates were isolated at appropriate embryonic stage. Protein isolation was performed with Tri-reagent solution (Ambion) according to manufacturer's advice. Proteins were separated on sodium dodecyl sulphate–polyacrylamide gels and then transferred to polyvinylidene fluoride microporous membranes (Immobilo-P transfer membrane, Millipore). The primary antibody used against Scrt2 was rabbit polyclonal anti-Scrt2 (P-20, Santa Cruz Biotech). Primary antibody used for equal loading control was rabbit polyclonal anti-β-tubulin (Covance). Blots were visualized with SuperSignal West Pico Chemiluminescent Substrate (Pierce Biotechnology), exposed on CL-XPosure clear blue X-ray film (Thermo Scientific), and developed using the Curix-60 Agfa system (Agfa Healthcare GmbH). The estimation of the fold difference between wild-type and Scrt2 overexpression conditions was assessed by calculating the density of pixels of the relative bands, using the GS-800 calibrated densitometer (Bio-rad) and the Quantity one 4.6.9 1-D analysis software.

Cell Transfection and Luciferase-Reporter Assay

Transient transfection of HeLa or P19 cells cultured in Dulbecco's modified Eagle medium (DMEM) medium plus 10% fetal calf serum was performed using Lipofectamine2000 (Invitrogen) and endotoxin-free DNA plasmids (Qiagen Kit) according to the supplier's

guidelines. Dual-luciferase-reporter assay (Promega) was done 24 h after transfection and firefly luciferase activity was normalized to Renilla luciferase-reporter activity. Data shown represents the mean of 3 separate experiments with values present as *Scrt2GOF*/control ratios (shown as mean ± standard error of the mean [SEM]).

In Utero Electroporation

IUE was performed according to Tabata and Nakajima (2001) using 2 μg/μL endotoxin-free DNA plasmids (EndoFree Plasmid Kit, Qiagen). For *Scrt2* gain of function experiments, empty GFP expression plasmid (*pCIG2* = *CMV-GFP*), or expression plasmids containing codon-optimized open reading frame (Supplementary Fig. S2*C*) of *Scrt2* (*CMV-Scrt2-GFP*), was injected and electroporated in the lateral ventricle of E13.5 or E14.5 embryos, using the ElectroSquarePorator ECM 830 (BTX) set to five 50 ms pulses at 30–35 V. In rescue experiments of the migrational phenotype, the *Scrt2-GFP* expression plasmid was coinjected with *CMV-Rnd2-GFP* expression vector (Heng et al. 2008) in a molar ratio of 1:1. Embryos were sacrificed at stage E16.5, E18.5, or P2 and processed for IHC. Cells marked by the expression of GFP were counted manually to determine the percentage of the electroporated cells in each cortical compartment visualized with DAPI staining. For *Scratch2* knockdown (KD) experiments, 4 shRNA-Scratch2 sequences containing turbo-GFP reporter were purchased from Origene. Two of these constructs were able to suppress up to 2-fold the endogenous Scratch2 expression in P19 cells in vitro. It should be noted that turbo-GFP was very faintly expressed and subsequent immunostaining with turbo-GFP antibody did not improve the signal. Therefore, in order to facilitate our experimental conditions, IUEs for Scrt2KD were performed in E13.5 embryo brains with either a control shRNA plasmid (2.5 μg/μL) plus pCIG2-GFP empty vector (0.7 μg/μL) or shRNA-Scrt2 plasmid (2.5 μg/μL) plus pCIG2-GFP vector (0.7 μg/μL).

Pair-Cell Analysis

Pair-cell analysis was performed as described by Bultje et al. (2009). Targeted GFP+ regions of cortices from electroporated E13.5 embryos were dissected at E14.5, trypsinized, and mechanically dissociated to generate a homogeneous cell culture. The cells were plated on poly-D-lysine-coated chamber slides (Lab-Tek) in FGF2- (10 ng/mL) supplemented culture medium (DMEM + glutamine with 2% B27, 1% N2, 1% penicillin/streptomycin). After 24 h incubation, pair cells were identified by fixing with 4% PFA and double immunostained overnight at 4°C with antibodies using ck α-GFP, 1:500 (Abcam) and sequentially, rb α-Pax6 (Covance), 1:300; rb α-Tbr2 (Abcam), 1:300; or ms α-Tuj, 1:500 (Covance). Secondary Alexa 488 α-ck and Alexa 568 α-rb/ms (1:500, Invitrogen) were applied for 2 h at room temperature, and the slides were covered in DAPI solution. More than 200 cell pairs per experimental condition were counted ($n = 3$).

Image Analysis, Quantification, and Statistical Analysis

Images were captured with an Olympus BX60 fluorescent microscope, an Olympus SZX 12 fluorescent binoscope, or a laser confocal microscope (Leica Sp5). Cell counting at stages E12.5 and P10 was done blind to the animal genotype on every 10th section including the dorsal pallium (for E12.5) or the cortex (for P10). A frame of 500 μm (for E12.5) or 1000 μm (for P10) encompassing the entire cortical plate (CP) was applied. For stage E12.5, the frame was placed as shown in Figure 4*B*1. For stage P10, the frame was placed within the somatosensory cortex. For additional cell counts in sections from E12.5 (Supplementary Fig. 4) and E16.5 brains (Fig. 5), cells within equally sized fields in dorsal or lateral pallium of the control or double transgenic animals were counted at rostral and caudal levels (as indicated in the histograms). Similarly, equally sized frames were positioned onto electroporated hemispheres, and GFP+ cells were counted in respective cortical zones/layers. Radial cortical zones were defined by their characteristic cell densities of DAPI staining. For perikaryon measurements of Neurofilament Smi32-stained L5 neurons, the longest diameter of at least 90 cells per genotype visualized under high magnification by confocal microscopy was measured by the Leica LAS software, the processes being excluded from the measurement. All images were processed with Adobe Photoshop (Version CS2) by overlaying the pictures, adjusting brightness, contrast, and size.

Xenopus Microinjections and Analysis

The optimized coding sequence for murine Scrt2 was PCR amplified and subcloned into GR-pCS2+. Capped mRNAs for microinjections were in vitro transcribed (*SP6* mMessage mMachine™; Ambion) and purified over an RNeasy column (Qiagen) using *Not1* linearized templates. Embryos were injected into 1 blastomere of the 2-cell stage with pg of *Scrt2*-GR, 25 *Ngn2*-GR, 100 GFP, and 50 nuclear *lacZ* mRNA as a lineage tracer. Embryos were incubated with dexamethasone (4 μg/mL in 0.1× MBSH) at various stages until fixation (Kolm and Sive 1995). X-gal staining (Hardcastle and Papalopulu 2000) and whole-mount in situ hybridization were performed essentially as described (Harland 1991) using antisense RNA labeled with DIG-11-uridine triphosphate (DIG)-11-UTP prepared from the following constructs: *Sox3* (Klisch et al. 2006); *Ngn2/Ngnr-1* (Ma et al. 1996); *MyT1* (Bellefroid et al. 1996); *N-tubulin* (Chitnis 1995); and GFP (Rubenstein et al. 1997).

Results

Expression of Scrt2 in the Developing and Adult Brain

Whole-mount ISH analysis with a *Scrt2*-specific antisense riboprobe revealed restricted expression in the developing central nervous system of the E12.5 mouse embryo (data not shown), and a robust accumulation of *Scrt2* transcripts in the upper zone of the SVZ and IZ of the E15.5 pallium (Fig. 1*A*1, *A*2), consistent with previous studies (Marin and Nieto 2006). A weak Scrt2-positive signal was also observed at the apical ventricular surface after a longer (48 h) color development (arrowhead, Fig. 1*A*2), while the expression in the intermediate zone (IZ) and E15.5 CP was stronger, being even more pronounced in CP of the newborn brain (P0, Fig. 1*A*3), as also reported by Marin and Nieto (2006). By dual ISH, *Scrt2* expression colocalized in the upper SVZ/IZ with the expression of *NeuroD1*, a marker of early differentiating neurons (Schwab et al. 1998; Cho and Tsai 2004) and partially with the IP marker *Tbr2* (Fig. 1*C*1,*C*2). The latter was also confirmed by ISH for Scrt2 and IHC for Tbr2 on adjacent sections from E15.5 wild-type brains (Fig. 1*C*3,*C*4). As an intrinsic determinant of the cortical RGPs (Götz et al. 1998), Pax6 exerts a leading role in the TF cascade: Pax6—Tbr2—Tbr1, which is involved in the generation of cortical glutamatergic neurons (Englund et al. 2005). Interestingly, in Pax6 deficiency, as opposed to the control, expression of *Scrt2* in the E15.5 embryo cortex of homozygous *Pax6*/*Small eye* mutant (*Sey*/*Sey* allele, Hill et al. 1991) was abolished in the dorso-lateral pallium (Fig. 1*D*1,*D*2). An almost identical defect in the regionalization pattern has been reported in the *Sey*/*Sey* embryonic cortex for the expression of TF *Ngn2*, which is a direct target of *Pax6* and has an important role in neuronal differentiation (Stoykova et al. 2000; Scardigli et al. 2001; Marin and Nieto 2006). Because of the peculiar punctuate immunopositive signal in the Scrt2 IHC, we carefully evaluated the specificity of the immunostaining. Observation under high magnification and using laser scanning confocal microscopy revealed that, while most of the punctate Scrt2 signal is cytoplasmic and colocalizes with β-catenin at the apical VZ surface (Fig. 1*H*1–*H*3), a granular Scrt2 immunolabeling is also observed in the nucleus (Fig. 1*H*1,*H*3, arrowheads). The staining was abolished by preincubation of the

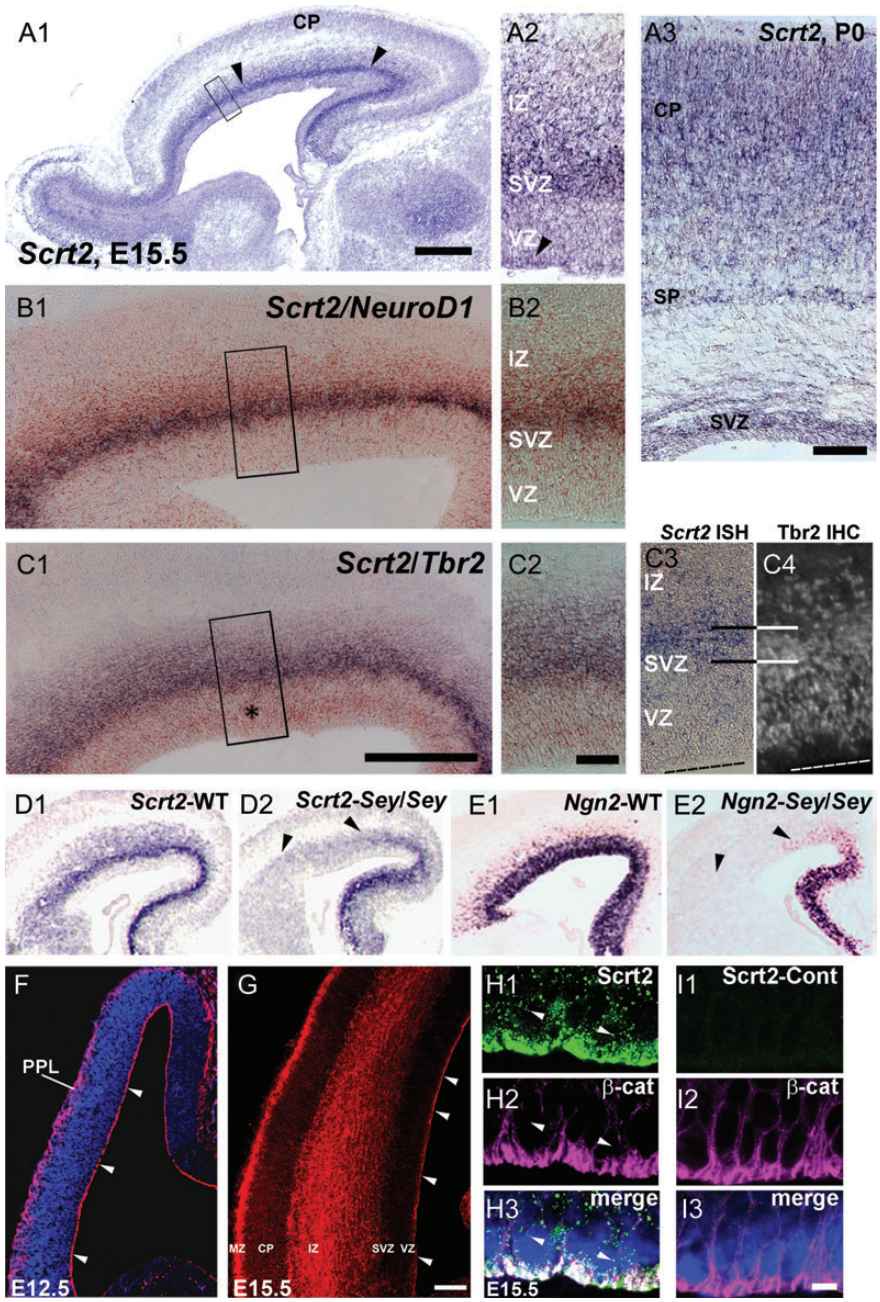

Figure 1. Expression of Scrt2 in the developing mouse cortex. (*A1–A3*) ISH with *Scrt2* in situ probe on sagittal brain sections at E15.5 (*A1*), P0 (*A3*), and a higher magnification image of a sagittal E12.5 section after a long (48 h) staining (*A2*) demonstrates a strong signal in the upper SVZ/IM zone (arrowheads), and a moderate or faint signal in the CP (*A1*), or at the ventricular surface (*A2*, arrowhead in VZ), respectively. At P0, *Scrt2* expression becomes stronger in the upper CP (*A3*). (*B1* and *C2*) Double ISH analysis for *Scrt2* and either *NeuroD1* (*B1*, *B2*—higher magnification image) or *Tbr2* (*C1*, *C2*—higher magnification image) (Scrt2-blue-AP and Tbr2/NeuroD-brown-DAB). Note the partial overlapping between *Scrt2* and *Tbr2* transcripts only in the upper SVZ/IZ, but not in the VZ (*). (*C3* and *C4*) Adjacent cross E15.5 brain sections were hybridized either with *Scrt2* in situ probe (*C3*) or were stained with Tbr2 antibody (*C4*). Note the partial overlapping of the signals only in the upper SVZ/IZ. (*D1–E2*) The regionalized loss of *Scrt2* expression in the dorsolateral pallium of Pax6$^{Sey/Sey}$ E15.5 embryos (*D1* and *D2*) is reminiscent of the regionalized inhibition of the expression of basic helix loop helix (bHLH) TF *Ngn2* in this mutant (shown in *E1*,*E2*). (*F* and *G*) Scrt2 immunostaining (counterstained with DAPI in blue) on E12.5 (*F*) and E15.5 (*G*) brain sections. The arrowheads point to Scrt2 expression at the apical surface of the VZ. (*H1–I3*) Confocal images (taken with a ×63 immersion objective) after double IHC with Scrt2 (*H1*) and β-catenin antibody (*H2*) of E15.5 brain sections depicts cytoplasmic colocalization of Scrt2/βcatenin at the ventricular surface, and the presence of Scrt2-positive punctata (arrowheads) in the nucleui (as depicted by DAPI staining). (*I1–I3*) In control stainings, the presence of a blocking peptide abolishes both the types of Scrt2 immunostainig. The same pattern of expression was observed also with the tested second Scrt2 antibody (Sigma-Aldrich) shown in Supplementary Figure 3*A1–B3*. Bars: 200μm (*A1* and *C1*), 20 μm (*C2*), 100 μm (*G*), 5 μm (*I3*).

primary antibody with a specific blocking peptide or omission of the primary antibody (Fig. 1*H1/I1*; *H3/I3* and Supplementary Fig. 3*E,F*), and a second commercially available antibody recapitulated the staining pattern (Supplementary Fig. 3*A1–A3*; see *B1–B3* for a control staining pattern). In agreement with the data from the ISH analysis (Fig. 1*D1,D2*), IHC on E15.5 *Sey/Sey* cortical sections showed almost a complete loss of immunostaining in the dorsolateral pallium (Supplementary Fig. 3*C,D*), thus demonstrating specificity of the immunosignal. Snail TFs have been found to be localized only

to a few chromatin foci in the nucleus, which are assumed to be sites of active RNA splicing, and in the cytoplasm of some cell lines (Dominguez et al. 2003, Yamasaki et al. 2005). Interestingly, cortical cells electroporated in vivo with CMV-Scrt2 expression vector via IUE revealed a robust nuclear immunostaining for Scrt2 (Supplementary Fig. 3*G–I*) suggesting the existence of a mechanism for nucleo-cytoplasmic transport of the Scrt2 protein.

We next attempted to define more precisely the Scrt2 expression in distinct types of cortical progenitors. Double IHC on brain sections at E13.5 and E15.5 showed colocalization of Scrt2 in apically dividing phosphorylated-Vimentin (p-Vim)-positive RGPs (Fig. 2*A1–A3*), almost all of which represent RGPs expressing the TF Pax6 (Fig. 2*B1–B3*). As recently shown, Insm-1 is a master regulator of IP genesis (Farkas et al. 2008). In the SVZ at E13.5, Scrt2 was expressed in dividing Insm1+ IPs (Scrt2+/Insm1+/3H3+; Fig. 2*C1–C4*) and in neurogenic IPs (Scrt2+/Insm1+/Ngn2+; Fig. 2*D1–D4*). To evaluate Scrt2 expression in subsets of IPs, double immunostaining for Scrt2/Tuj1 and Tbr2/Tuj1 was performed on adjacent E13.5 brain sections. We found a nearly complete Scrt2/Tuj1 colabeling in the upper SVZ and SVZ/IZ (Fig. 2*E1*, *E2*). Only a subset of Tbr2+ cells in the SVZ/IZ expressed Tuj1 (Fig. 2*F1*, white arrowheads), while in the lower SVZ, the Tbr2+ cells were negative for Tuj1 (Fig. 2*F1*,*F2*, black arrowheads). Thus, Scrt2 appears to be predominantly

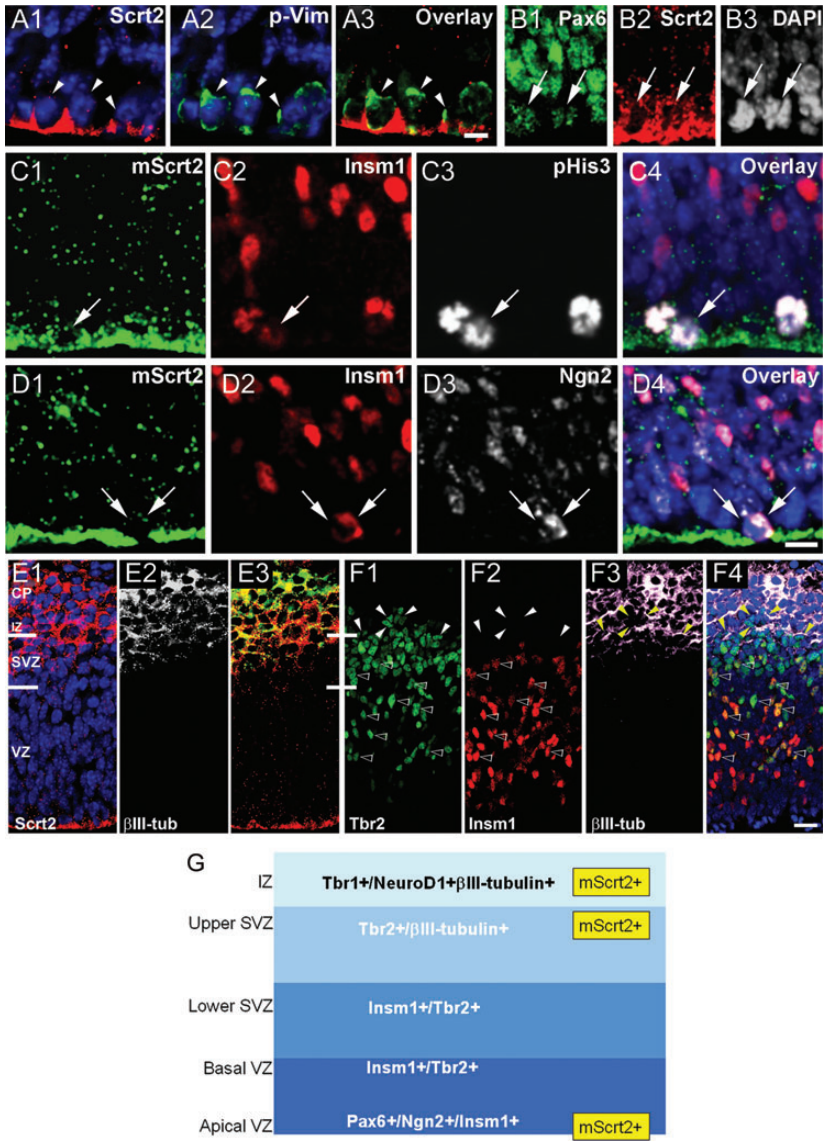

Figure 2. Cellular localization of Scrt2 in the developing mouse cortex. IHC analysis was performed on E13.5 and E15.5 (*B1–B3*) brain cross sections with the indicated antibodies. Single-channel images are presented in green, red, or white. (*A1–A3*) Double immunostaining with anti-Scrt2 and phosphorylated-Vimentin (p-Vim) antibodies shows expression of Scrt2 in apical dividing cortical progenitors. (*B1–B3*) Double IHC for TF Pax6 and Scrt2 shows that dividing apical Pax6+ RGPs (mitotic figures seen on DAPI staining in *B3*) express Scrt2 (arrows). The Scrt2 immunofluorescence has a punctuate appearance in the nucleus and a more homogeneous staining in the cytoplasm. (*C1–C4*) Subsets of Scrt2+ dividing cells in the VZ are IPs (arrows), double positive for TFs Insm1, and the mitotic marker phosphorylated H3 histone (pHis3). (*D1–D4*) Expression of Scrt2 in subsets of neurogenic Insm1+/Ngn2+ IPs. (*E1–E3*) Co-expression of Scrt2 in βIII-tubulin+ cells (IPs or young differentiated neurons) in the upper the SVZ/IZ and CP, respectively. The merged image in D3 illustrates that almost all βIII-tubulin+ cells are also Scrt2+. (*F1–F2*) IHC on adjacent to the section shown in *E* shows that in the VZ, Tbr2+, Insm1+, or Tbr2+/Insm1+ IPs (black arrowheads) do not colocalize with Scrt2 (compare with *D1*), and with βIII-tubulin (*E3*). (*F3–F4*) However, in the upper SVZ/IZ, Tbr2+/Insm1− IPs (white arrowheads in *F1*,*F2*) co-localize with Scrt2/βIII-tubulin signal (yellow arrowheads in *F3*,*F4*). (*G*) Schematic presentation of the cellular localization of Scrt2 in the germinal/IZ zones of the developing mouse cortex. Bars: 5 μm (*A1–B3*), 10 μm (*C1–D4*), 20 μm (*E1–F4*).

expressed in differentiating Tbr2+ cells in the upper SVZ and SVZ/IZ (Fig. 2*F*). However, the Tbr2+/Insm1+ subset of IPs (Farkas et al. 2008) did not express Scrt2 (compare Fig. 2*F*1, *F*2, black arrowheads, with *E*1).

In summary, our results show that, during mouse corticogenesis, TF Scrt2 is expressed in subsets of: 1) dividing RGPs at the apical surface at a time they are fated to produce either early neurons or IPs; 2) neurogenic Insm1+ IPs at SVZ and SVZ/IZ; 3) differentiating Tbr2+/Tuj1+ neurons in the upper SVZ and IZ, and 4) more abundantly in the upper cortical layers of the postnatal cortex. Together, these expression data strongly suggest that Scrt2 may play a role in the initiation and/or modulation of neuronal differentiation of glutamatergic cortical neurons.

Overexpression of Scrt2 Inhibits Primary Neurogenesis in Xenopus Embryo

In a first approach to analyze the function of Scrt2 during the development of the vertebrate nervous system, we performed gain-of-function (GOF) experiments in *Xenopus* embryos where the first neurons are already born shortly after gastrulation (Lamborghini 1980). These so-called primary neurons first arise in 3 bilateral stripes within the posterior open neural plate where members of the Neurogenin family of bHLH TFs act as neuronal determination factors within the neuroepithelium (Ma et al. 1996). Several variants of mammalian Scratch2 were previously predicted by in silico analysis from a common genomic locus (National Centre for Biotechnology Information), including Scrt2.2 (XM_619828.2), recently termed Scrt2 (NM_001160410.1), and analyzed in our study (Supplementary Fig. 1). To control the onset of protein activity, a hormone-inducible version of Scrt2 was generated by C-terminal fusion of the ligand-binding domain of the glucocorticoid receptor (GR; Gammill and Sive 1997). Murine *Scrt2-GR* mRNA was injected into 1 blastomere of 2-cell stage embryos together with *LacZ* mRNA to localize the distribution of the injected mRNA. At the onset of gastrulation, the injected embryos were treated with dexamethasone to induce Scratch2 protein activity. The influence of *Scrt2-GR* mRNA on the expression of neuron-specific class II *β-tubulin* (*N-tubulin*), a marker for postmitotic neurons, was evaluated by whole-mount in situ hybridization of stage 14 embryos. Neuronal differentiation was inhibited on the injected side of the embryo, as shown by the loss of *N-tubulin* expression (Fig. 3*A*4). This was not due to the loss of the neural progenitor cells, as *Sox3* expression was maintained (Fig. 3*A*1). Overexpression of *Scrt2-GR* also inhibited the expression of the proneural determination gene *Ngn*2 (Fig. 3*A*2), but the loss of expression was not as strong of that observed for the *Ngn2*-downstream target gene *MyT1* (Fig. 3*A*3) or *N-tubulin*. As a control, GFP mRNA was also injected and did not influence the expression of any of the markers genes evaluated (Fig. 3*A*5–*A*8). These results suggest that Scrt2 inhibits the downstream activities of the proneural factor Ngn2 and to a lesser extent its expression.

Conditional Activation of Scrt2 in Cortical Progenitors in Transgenic Mice Diminishes the Number of Neurons in the Mature Cortex

The Scrt2 expression pattern in the developing mouse pallium, and the strong inhibition of the primary neurogenesis upon activation of *Scrt2* in *Xenopus* embryo, motivated us to examine whether, and if so how, is Scrt2 involved in cortical neurogenesis. As most of the Snail family members, including the mammalian Scratch1, act as repressors (Hemavathy et al. 2000; Nakakura et al. 2001), we applied an in vivo GOF approach to study the function of *Scrt2* after gene activation in the developing cortex of transgenic mice (Berger et al. 2007). Based on the Cre-loxP recombination strategy, a mouse line (*JoScrt2*) was generated with a floxed *Scrt2* allele, allowing conditional gene expression (Supplementary Fig. 2*A*). Male *JoScrt2* founders were crossed with female animals of the *Emx1Cre* line (Gorski et al. 2002), which drives Cre-recombinase activity in the cortical progenitors, starting at E9.5 and reaching full recombination at E12.5 in most proliferating pallial progenitors and their postmitotic descendants (Li et al. 2003; Armentano et al. 2007; Berger et al. 2007; Supplementary Fig. 2*D*1–*E*2). IHC analysis at E12.5 showed enhancement of the Scrt2 immunosignal in the pallium (Supplementary Fig. 2*F*1,*F*2). Western blot of cortical lysates at E15.5 revealed that, compared with the control, the *JoScrt2*; *Emx1-Cre* cortex contained almost a 2-fold higher amount of Scrt2 protein (Supplementary Fig. 2*G*), demonstrating that the applied strategy produces a mild Scrtach2 overexpression in vivo.

DAPI-stained sections from P10 brains of the mutant double transgenic *JoScrt2*; *Emx1Cre* mice revealed a moderate, but statistically significant thinning of the mutant cortex when compared with the control (Fig. 3*B*1–*B*3). IHC staining with an antibody for active caspase-3 on brain sections at E12.5, E16.5, and P10 did not show any significant difference in apoptosis between the *Scrt2GOF* and control cortices (data not shown). At P0, we observed intensive Scratch2 expression in the upper zone of the CP and coimmunostaining with Satb2, an UL neuronal marker (Alcamo et al. 2008; Britanova et al. 2008; Fig. 1*A*3 and data not shown). To assess whether, in the *Scrtach2GOF* mutant, there is a selective loss of neuronal subtypes, we employed layer-specific molecular markers. IHC with an anti-Cux1 antibody that specifically labels UL neurons (Nieto et al. 2004; Zimmer et al. 2004) revealed a diminishing of the UL neuronal density, especially at caudal levels, compared with the control (Fig. 3*C*1–*C*5). Immunostaining for the LL marker Ctip2 (Arlotta et al. 2005; Molyneaux et al. 2005, 2007) disclosed no significant change in the density of Ctip2+ cells in L6 (Fig. 3*D*1,*D*3 and data not shown). However, we observed increased numbers of Ctip2+ cells specifically in L5 of the mutant cortex (Fig. 3*D*1–*D*5). L5 Ctip2+ neurons are generated preferentially through direct neurogenesis from RGPs, thus, their increase in the Scrt2 mutant is reminiscent of supernumerary neurons generated upon ectopic expression of *Drosophila* Scrt in neuronal progenitors (Roark et al. 1995). Furthermore, labeling with the neurofilament (NF-H) antibody Smi-32, a specific marker for L5 pyramidal neurons, revealed that the diameter of these cell perikarions was about 18% smaller in the *Scrt2GOF* caudal cortex (Fig. 3*E*1–*E*3). Thus, transgenic Scrt2 overexpression in RGPs and their descendants seems to affect differently the generation of early- and late-born neurons.

To determine whether the *Scrt2GOF* forces neuronal differentiation during early neurogenesis, we performed expression analysis on E12.5 brain sections from *JoScrt2*; *Emx1Cre* and control embryos. IHC with a Pax6 antibody, which marks the apical RGPs (Götz et al. 1998), and an antibody for bHLH TF

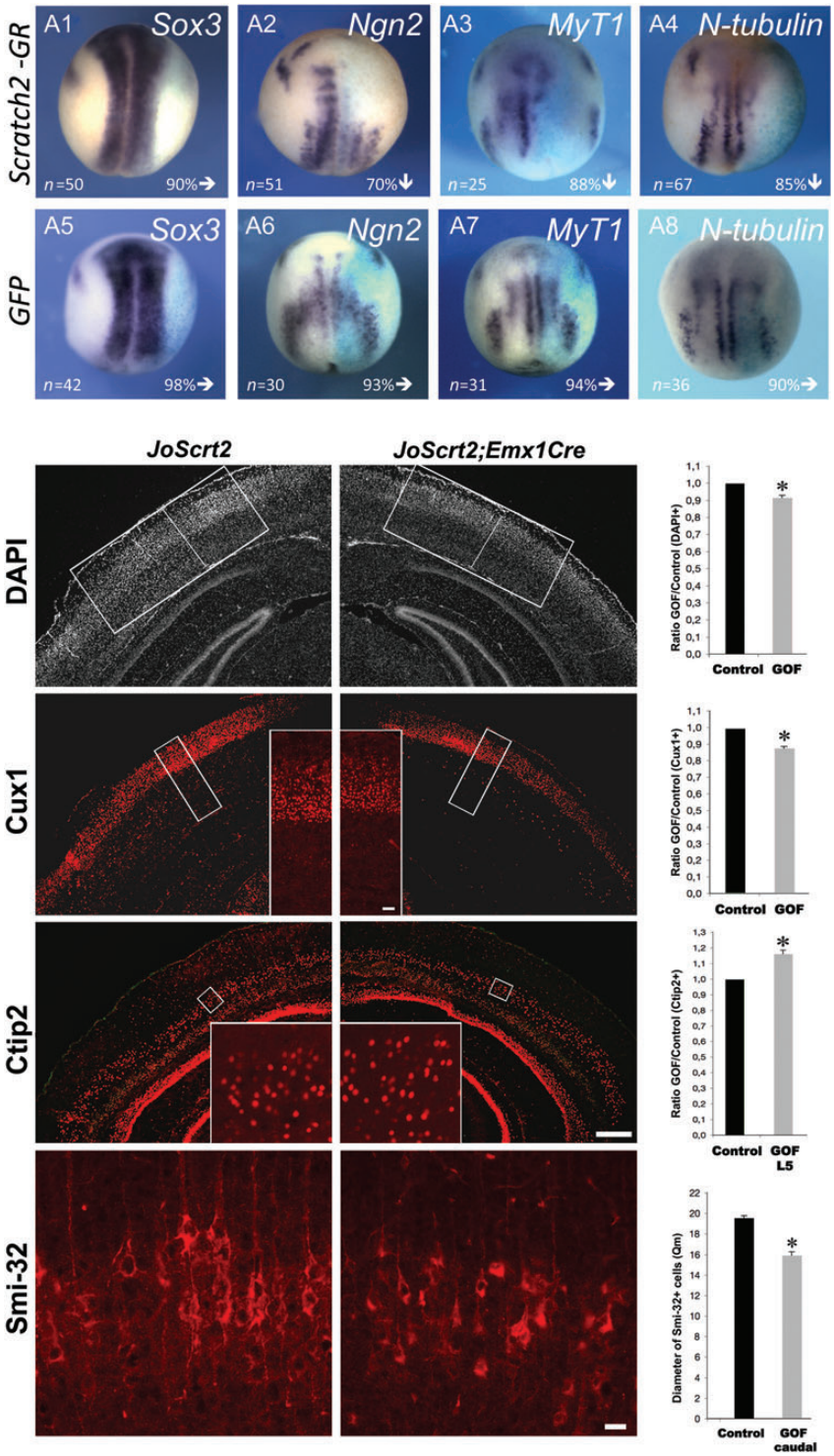

Figure 3. Overexpression of mammalian *Scrt2* causes inhibition of the primary neurogenesis in *Xenopus* embryos and reduction of cortical thickness in transgenic mice. (*A*1–*A*8) Whole-mount in ISH at stage 14 of *Scrt2-GR* (100 pg) and *GFP* mRNA-injected *Xenopus* embryos. The injected mRNA is indicated to the left and antisense probes used are indicated in the upper right. Embryos are shown as a dorsal view, anterior up and the injected side (β-gal, light blue) is always on the right side. Number of embryos analyzed and percent embryos showing the phenotype are indicated at the bottom. (*B*–*E*) IHC analysis on cortical sections of *Scrt2GOF* and control mice at P10. Images show matched cross sections at caudal level of control (*B*1–*E*1) and mutant (*B*2–*E*2) brain after staining as indicated. (*B*1–*B*3) DAPI histochemistry revealed a reduced thickness of the caudal mutant cortex when compared with the control cortex by 10% (*B*3). (*C*1–*C*5) IHC with anti-Cux1 antibody revealed diminishing of the ULs of the mutant when compared with the control. The frames in B1/B2 demonstrate the counting frames position for Cux1 IHC in *C*1/*C*2. *C*2 and *C*4 are higher magnification images from the pointed fields in *C*1 and *C*3, respectively. (*D*1–*D*5) The number of Ctip2+ neurons in L6 + L5 did not show a significant change, however, Ctip2+ neurons were increased in the mutant when compared with control cortex, when counted only in L5. *D*2 and *D*4 are higher magnification images from the pointed fields within layer5 in *C*1 and *C*3, respectively. (*E*1–*E*3) Staining with Smi-32 antibody revealed smaller diameter of L5 neuronal somas by 15% in the mutant when compared with the control. Quantifications were performed on brain sections of both genotypes at rostral and caudal levels on every 10th section in 3 independent experiments. Data (GOF/control ratio) are presented as mean ± SEM; $*P < 0.05$. Scale = 200 μm (*D*3), 20 μm (*E*2).

Ngn2, a downstream direct target of Pax6 (Scardigli et al. 2003) revealed a generally unaltered expression patterns in the *JoScrt2*; *Emx1Cre* mutant with respect to the control cortex (Supplementary Fig. 4*A*1–*C*2). IHC staining for T-box TF Tbr1, a specific marker of early-born preplate neurons at this stage (Hevner et al. 2001), revealed that, compared with the control, *Scrt2GOF* mice had an enlarged set of differentiated neurons (Fig. 4*A*1–*A*3). From E10.5 until E12.5, TF Tbr2 is expressed in βIII-tubulin (Tuj1)+ neurons of the preplate, including the Cajal–Retzius cells of the future marginal zone (Englund et al. 2005), as well as in a few early generated IPs in the germinative zone (Haubensak et al. 2004). In contrast to the control, at rostral and caudal levels, the *JoScrt2*; *Emx1Cre* cortex contained slightly enhanced number of Tbr2 + cells, mostly reflecting postmitotic preplate neurons (Fig. 4*B*1–*B*3). Consistent with the advanced differentiation of the lateral pallium, the set of double Tbr2+/Tuj1+ neurons in this region was significantly enlarged in the mutant with respect to control cortex (Fig. 4*C*1–*C*5). Expression of *Tis21* in cortical progenitors has been associated with the switch from progenitor proliferation to neurogenesis, thus being accepted as a marker for neurogenic progenitors (Haubensak et al. 2004). Using *Tis21* in situ probe, we found by ISH an increased presence of neurogenic progenitors in pallial VZ of E12.5 *SCrt2GOF* when compared with the control brain (Supplementary Fig. 3*D*1,*D*2). Together, these data suggest that overexpression of *Scrt2* at the onset of cortical neurogenesis promotes RGPs to more often undertake a neurogenic division, generating an excess of the earliest-born preplate and early-born LL neurons.

To further test this possibility, pregnant mice at E12.5 were BrdU pulse-labeled and analyzed 24 h later, thus approximately after 1 mitotic cycle of RGPs at this stage. IHC analysis of the CP differentiation showed that, compared with the

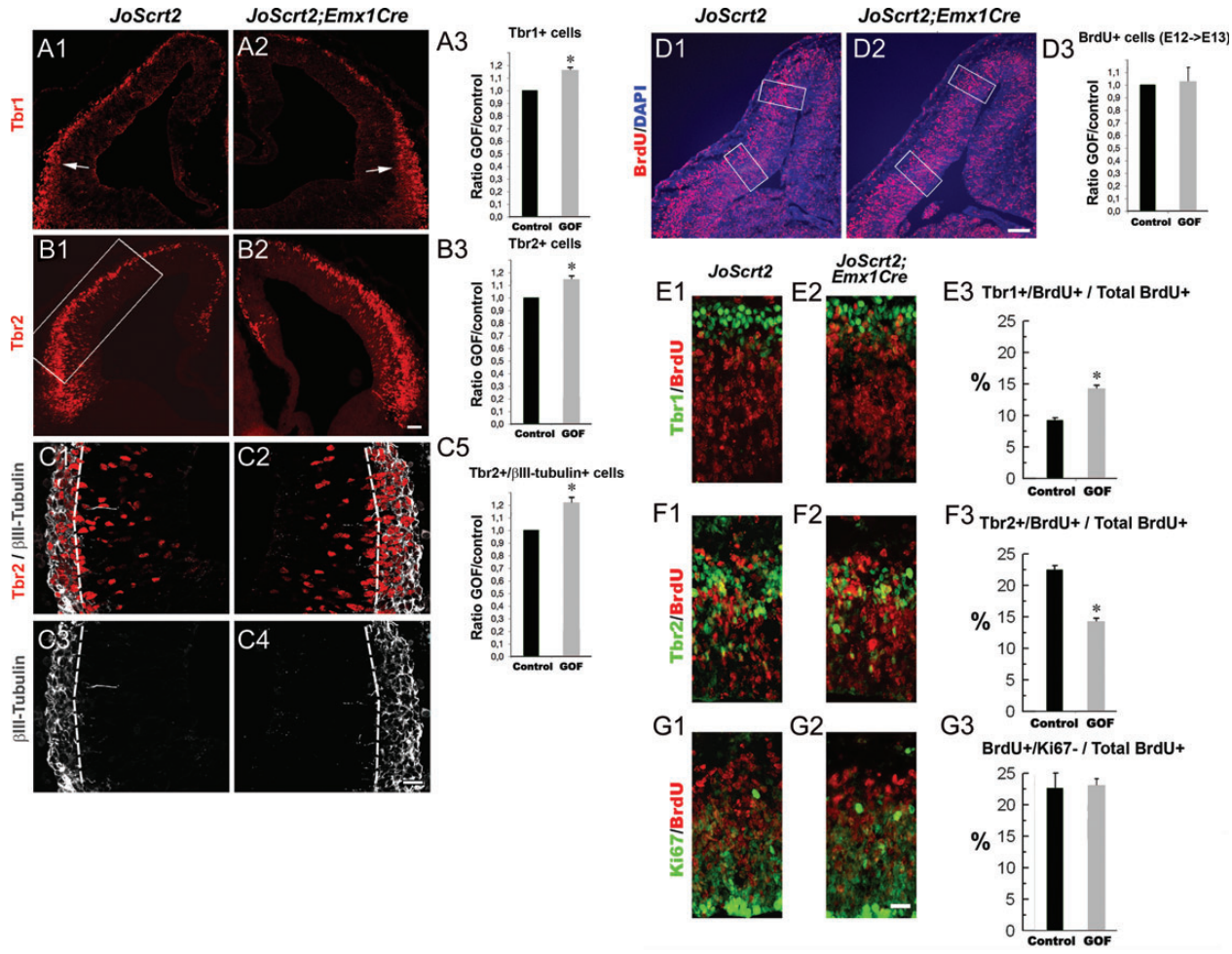

Figure 4. Enhanced early-born neuronal production in *Scrt2GOF* cortex at E12.5. IHC analysis was performed on cross sections from control (*JoScrt2*) and mutant (*JoScrt2*; *Emx1Cre*) brains. (*A*1–*B*2) In E12.5 dorsal pallium, a 0.5-mm long frame for counting was used (shown in *B*1) to count early-born preplate neurons that are immunopositive either for Tbr1 (*A*1 and *A*2) or Tbr2 (*B*1 and *B*2) on every 10th section (systematic random sampling). (*A*3 and *B*3) Compared with the controls, preplate neurons were produced in a slight excess in *Scrt2GOF* pallium. (*C*1–*C*5) Double IHC with Tbr2 and βIII-tubulin antibody in the lateral pallium (frame in *D*1), where CP differentiation is already initiated at this stage, revealed an enhanced number of preplate/CP neurons in *Scrt2GOF* cortex. (*A*3, *B*3, and *C*5) The histograms represent the mean values (mutant/control) after cell countings in equallysized frames (in *B*1) from 3 experiments; mean ± SEM; $*P < 0.05$. Scale = 25 μm (*A*2), 50 μm (*B*1–*D*2), 20 μm (*E*2). (*D*1–*D*3) After in vivo BrdU pulse labeling of E12.5 embryos for 24 h, the number of proliferating cells in the dorsal pallium was not changed in the *Scrt2GOF* mutant when compared with the control. Measurements were done in dorsal and lateral pallium in frames as depicted in *D*1/*D*2. (*E*1–*G*3) In the same experiment, matched sections from control and *Scrt2GOF* E13.5 brains were double immunostained for BrdU with either Tbr1, Tbr2, or Ki67 antibodies. Countings indicated that for approximately 1 cell cycle, in *Scrt2GOF* embryos, is generated an increased number Tbr1+/BrdU+ dual-labeled neurons (*E*3) and a reduced number Tbr2+/BrdU+ cells (IPs and preplate neurons). The proportion BrdU+/Ki67− versus total Brdu+ immunolabeled cells did not reveal differences to the controls in the cell cycle exit at this stage (*G*3).

controls, the Scrt2 overexpression increased the proportion of Tbr1+ LL neurons (Fig. 4*E*1–*E*3), while the generation of Tbr2 + cells was suppressed (Fig. 4*F*1–*F*3). Both cell proliferation measured by BrdU/DAPI dual labeling (Fig. 4*D*1–*D*3) and cell cycle exit measured by BrdU/Ki67 double staining (Fig. 4*G*1–*G*3) revealed no difference between the control and mutant cortex. Altogether, these results suggest that, at early stages of mouse cortical development, *Scrt2GOF* in vivo favors the direct mode of neurogenesis without altering the proliferation and cell cycle exit of progenitors.

Given the robust endogenous Scrt2 expression in the pallial SVZ/IZ at mid-corticogenesis, we studied the effect *Scrt2GOF* in cortical development at E16.5. At this stage, the neurons are generated predominantly via the indirect mode of neurogenesis, utilizing Tbr2+ IPs as amplifiers of generated neuronal fates. At E16.5, as at E12.5, the expression for both Pax6 and Ngn2 was unaltered in the mutant (Fig. 5*A*1–*B*2,*G*, *H*). However, the number of the Tbr2+ IPs, located either in the germinative zone (VZ plus SVZ) or the IZ, was clearly diminished in the *JoScrt2*; *Emx1Cre* cortex: In VZ/SVZ, a decrease by 23% rostrally and 9% caudally; in IZ, by 27% rostrally and 38% caudally (Fig. 5*C*1/*C*2,*G*,*H*). The results suggest a reduced generation of Tbr2+ IPs from RGPs in an *Scrt2GOF* condition, or preference of IPs to undergo neurogenic instead of proliferative division in the SVZ/IZ. Supporting the last possibility, IHC with an anti-pH3 antibody indicated a significant loss (49% rostrally and 55% caudally) specifically in basally dividing IPs in the mutant SVZ, while the apical RGPs seemed to proliferate normally (Fig. 5*D*1/*D*2, *G*,*H*).

To evaluate whether the cell cycle exit was affected during the late neurogenesis, pregnant mice of both genotypes were pulse labeled with CidU at E14.5 and 24 h later, and sections from E15.5 cortices were analyzed after double immunostaining with CidU and Ki67 antibodies. We found that, compared with the control, the *Scrt2GOF* mutant exhibited an enhanced exit of progenitors from the mitotic cycle as defined by the number of CidU+/Ki67− cells out of the total CidU+ cells (Supplementary Fig. 6*A*–*C*). In contrast, cell proliferation as measured by a 2-h IdU pulse at E15.5 remained unchanged in the mutants (Supplementary Fig. 6*D*–*F*). These findings suggest that, during the peak level of endogenous *Scratch2* expression in the SVZ/IZ, *Scrt2GOF* induces premature cell exit leading to neurogenic divisions of the progenitors, and diminishing the IP pool.

We noticed that a portion of Tbr1+ and Ctip2+ LL neurons appeared to be delayed in their migration to the CP in the *Scrt2GOF* mutant cortex (arrows in Fig. 5*E*2,*F*2). Therefore, we analyzed the radial distribution of CidU+ cells across the cortex after 24-h CidU pulse labeling (E14.5–E15.5). Although the generated neurons are still underway, the analysis revealed an increased proportion of CidU-labeled cells in the deep bins (bins 3 and 4, corresponding to the SVZ) of the mutant dorsal pallium, while a decreased proportion of the labeled cells was observed in the superficial bins (corresponding to the CP) of the mutants (Fig. 5*I*1–*I*3). These data suggested a migrational problem upon *Scrt2GOF* that seems to affect more strongly the UL neurons. The above observations are further supported by the expression analysis performed at E18.5 with UL-specific neuronal markers indeed revealing prominent sets of retained cells in the SVZ of the mutants, positive for the *Cux2* (Fig. 5*J*1,*J*2), *Math2/Nex* (Fig. 5*K*1,*K*2), and *FoxG1* (Fig. 5*L*1,*L*2). Overall, these findings support a role for Scrt2 in the migration of postmitotic neurons to the CP.

Overexpression of Scrt2 Promotes Neurogenic Progenitor Division

To investigate in a quantitative manner if overexpression of *Scrt2* indeed promotes a direct versus indirect mode of cortical neurogenesis, we performed a forced overexpression of *Scrt2* via IUE into the embryonic brain followed by clonal pair-cell assays in vitro (Shen et al. 2002; Bultje et al. 2009; Fig. 6*A*). E13.5 brains were electroporated with Scrt2 (*CMV-Scrt2-GFP*) or control (*CMV-GFP*) expression vectors. One day later, cortices were dissected, dissociated, and cultured in vitro for 1 day in FGF2-supplemented medium (DIV1), at a clonal density that allows proliferation (Bultje et al. 2009), followed by IHC analysis.

As a specific marker for RGPs, the expression of TF Pax6 in both cells of a clonal pair reflects their proliferative symmetric division, whereas a clonal pair having only 1 Pax6+ cell (Pax6 +/−) represents an asymmetric division, with the negative cell being either an IP or a neuron. TF Tbr2 is strongly and specifically expressed in IPs, where it contributes to their proliferation and maintenance (Sessa et al. 2008). In the SVZ, the IPs undergo either proliferative divisions, to generate 2 or 4 IPs, or undergo terminal neurogenic divisions to generate neurons (Haubensak et al. 2004; Miyata et al. 2004; Noctor et al. 2004; Wu et al. 2005). The initiation of neuronal differentiation and generation of immature neurons in the SVZ are marked by a diminishing of the Tbr2 expression level, concomitant with a transient expression of the bHLH TF NeuroD1 (Englund et al. 2005). Accordingly, the proliferative divisions of IPs give rise to cell pairs showing equally strong Tbr2 labeling (Tbr2+/+), while cell pairs with only 1 Tbr2-strongly positive cell (Tbr2 +/−) are composed of an IP and a RGP. To detect postmitotic neurons in the clonal cell pairs (avoiding a misquotation of postmitotic cells that are faintly expressing Tbr2), IHC with Tuj1 antibody was included, which is the earliest marker for terminally differentiated neurons. Symmetric Tuj1 expression in both cells (Tuj1+/+) of the clonal cell pair indicates a generation of 2 neurons through a neurogenic IP division via the indirect mode of neurogenesis, whereas restricted Tuj1 expression to only one of the clonal partners (Tuj1+/−) indicates a neuron generated by asymmetric neurogenic division of RGP via the direct mode of neurogenesis.

Analysis of the symmetric proliferative RGPs divisions (Pax6+/+ pairs) showed that the proliferation of RGPs was not significantly altered (control: 42.0%, SEM 0.98; *Scrt2GOF*: 43.9%, SEM 0.97; $P = 0.79$; Fig. 6*B*). This finding is consistent with the shown above unchanged expression of Pax6 in RGPs in the *JoScrt2*; *Emx1Cre* transgenic embryos at E12.5 and E16.5. The fraction of asymmetric RGP divisions (Pax6+/− pairs) was increased by approximately 3.5-fold in the *Scrt2GOF* when compared with the control (control: 6.7%, SEM 0.82; *Scrt2GOF*: 23.7%, SEM 0.47; $P = 0.01$). Asymmetric RGP divisions can generate 1 neuron and 1 RGP (direct neurogenesis), or alternatively, 1 neuron and 1 IP (indirect neurogenesis). Therefore, we examined the expression of Tbr2 to distinguish between these 2 options. Notably, upon *Scrt2GOF*, the cell pairs with an asymmetric and strong expression of Tbr2 (the Tbr2+/− pairs, counting for asymmetric RGP divisions that generate 1 Tbr2+ IP and 1 RGP)

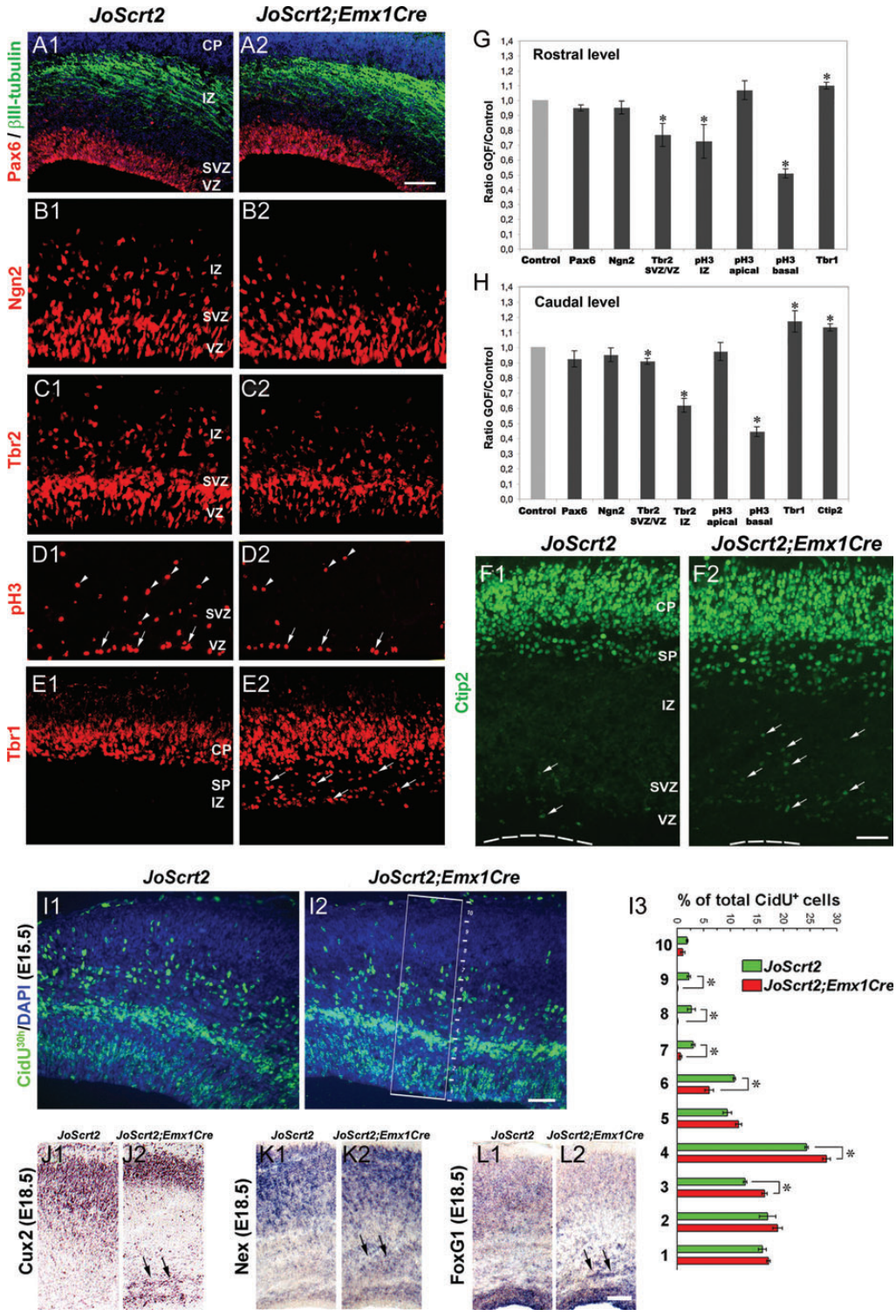

Figure 5. Enhanced direct neurogenesis and diminished IP pool in E16.5 *Scrt2GOF* cortex. (*A1*–*B2*) Immunofluorescence staining shows unchanged expression of the RGP marker Pax6 (*A1*/*A2*) and its downstream target Ngn2 (*B1*/*B2*). (*C1* and *C2*) Compared with the control, the *Scrt2GOF* cortex contains a diminished number of Tbr2+ IPs in the germinative (VZ + SVZ) plus IZ zones at rostral and caudal levels (quantified values in *G*,*H*). (*D1* and *D2*) Staining with pH3 antibody revealed a similar number of mitoses at the apical VZ surface (arrows), but significantly reduced number of abventricularly dividing progenitors (arrowheads, also *G*,*H*). (*E1*–*F2*) Enlarged number of Tbr1+ LL (*E1*/*E2*, *G*, *H*) and Ctip2+ L5 neurons (*F1*/*F2*, *H*) across the radial thickness of DP was detected in *Scrt2GOF* with respect to the control. The arrows in (*E2* and *F2*) point to LL neuronal sets possibly showing a migration delay in the mutant. (*G* and *H*) The histograms represent the mean values (mutant/control) after cell countings in equally sized frames (200 × 300 μm) in DP from 3 experiments and presented as mean ± SEM; $^*P < 0.05$. Bars: 100 μm (*A*) and 50 μm (*B*–*F*). (*I1*–*I3*) Immunostaining for CidU after 30 h in vivo labeling on E15.5 brain sections from control (*I1*) and mutant (*I2*) brains. On the images, the cortex was divided radially into 10 equally thick bins with bin 1 at the lowermost position and bin 10 at the uppermost position, and the percentage of CidU+ cells in each bin was estimated (*I3*). Note that compared with the control, in *Scrt2GOF* cortex, more labeled cells were trapped within the region of SVZ (bins 3 and 4), suggesting a migrational defect. (*J1*–*L2*) ISH analysis on cross E18.5 brain sections of control and *Scrt2GOF* mutant brain tested for expression of marker genes of lately-born UL neurons, including *Cux2* (*J1*/*J2*), *Math2*/*Nex* (*K1*/*K2*), *FogG1* (*L1*/*L2*), revealed the presence of retained beneath the CP cells in the mutant (arrows). Bars: 100 μm (*A2* and *L2*), 50 μm (*F2* and *I2*).

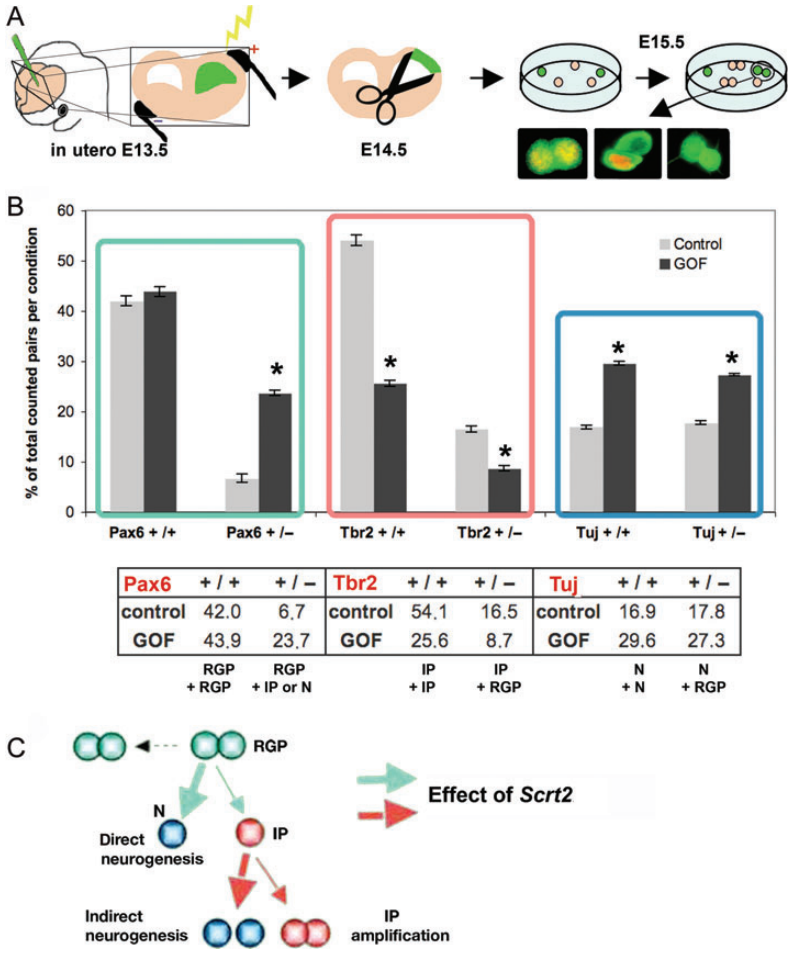

Figure 6. Overexpression of *Scrt2* in RGPs in vivo leads to enhanced premature neurogenesis at the expense of IP generation and amplification. (*A*) Schematic illustration of the clonal cell-pair assay. Embryos were in utero electroporated at E13.5 with a *Scrt2* CMV expression construct (*CMV-Scrt2-GFP*) or control vector (*pCIG2* = *CMV-GFP*). The next day, the CFP+ electroporated cortical tissue was dissected, dissociated, plated at clonal density, and maintained for 24 h in cultures. ICC analysis was performed with Pax6, Tbr2, or βIII-tubulin (Tuj1) antibodies (red), and anti-GFP antibody (green). (*B*) Each of the 3 applied markers was analyzed in GFP+ cell pairs and classified based on its expression in both cells (+/+), in only 1 cell (+/–) or in none of the GFP+ cell pairs, as described in more details in Results. The data in the histograms are shown as percentile values of total GFP+ analyzed cells per condition (means from 3 assays ± SEM.). (*C*) The schema illustrates effect of forced in vivo *Scrt2* expression on the mode of progenitor division. The symmetric proliferative division of RGPs (in green) is unaffected. However, *Scrt2GOF* favors asymmetric neurogenic divisions of RGPs (thick green arrow), generating a mild excess of neurons (N; blue) in a direct mode of neurogenesis (P → P + N) at the expense of generation of intermediate progenitors (IP; red) through an asymmetric progenitor division (P → P + IP). The IPs, instead of amplifying, undergo preferentially the terminal neurogenic division (thick red arrow), thus hampering neuronal fate amplification through the indirect mode of neurogenesis.

showed a 2-fold decrease in *Scrt2GOF* with respect to the control (control: 16.5%, SEM 0.58; *Scrt2GOF*: 8.7%, SEM 0.48; $P = 0.02$). Similarly, the number of cell pairs with strong and symmetric Tbr2 expression (Tbr2+/+ reflecting proliferative IP divisions) was clearly decreased (2-fold) in the *Scrt2GOF* (control: 54.1%, SEM 1.05; *Scrt2GOF*: 25.6%, SEM 0.63; $P = 0.01$). This is in accordance with a decrease in pH3+ mitotic cells in the *JoScrt2*; *Emx1Cre* cortex SVZ at E16.5 (Fig. 5*D*). Altogether, these data suggest that *Scrt2GOF* negatively influences IP proliferation and promotes the IPs to undergo premature neurogenic terminal division, which is reflected in the generation of a higher proportion of Tuj1+/+ clonal pairs in *Scrt2GOF* when compared with control (control: 16.9%, SEM 0.35; *Scrt2GOF*: 29.6%, SEM 0.34; $P = 0.007$).

Taken together, in agreement with the findings from the analyses of the transgenic *Scrt2GOF* mice, these data argue that overexpression of *Scrt2* in RGPs results in excess of early-born neurons through promoting the direct mode of neurogenesis (detected as Tuj1+/– pairs, control: 17.8%, SEM. 0.29; *Scrt2GOF*: 27.3%, SEM 0.25; $P = 0.005$). The preferable neurogenic division of both types of cortical progenitors (RGPs and IPs) leads not only to the production of fewer IPs, but also to an insufficient multiplication of the SVZ IPs, which diminishes neuronal constituents of the mature cortex as seen in the *Scrt2GOF* transgenic mice.

Should the ectopic overexpression of Scrt2 in cortical progenitors force the direct neurogenesis as suggested above, "KD" of the endogenous Scratch2 expression level would be expected to influence the neurogenesis preferably via Tbr2+ IPs. Therefore, we performed KD in vivo experiments via IUE of shRNA-Scrt2 in E13.5 embryo brains. Even though the shRNA-Scrt2 was able to only mildly deplete the *Scrt2* expression (up to 2-fold upon transfection of P19 cells), at E15.5, we found a substantial increase of GFP+/Tbr2+ cells (i.e. IPs and differentiating neurons in indirect neurogenesis;

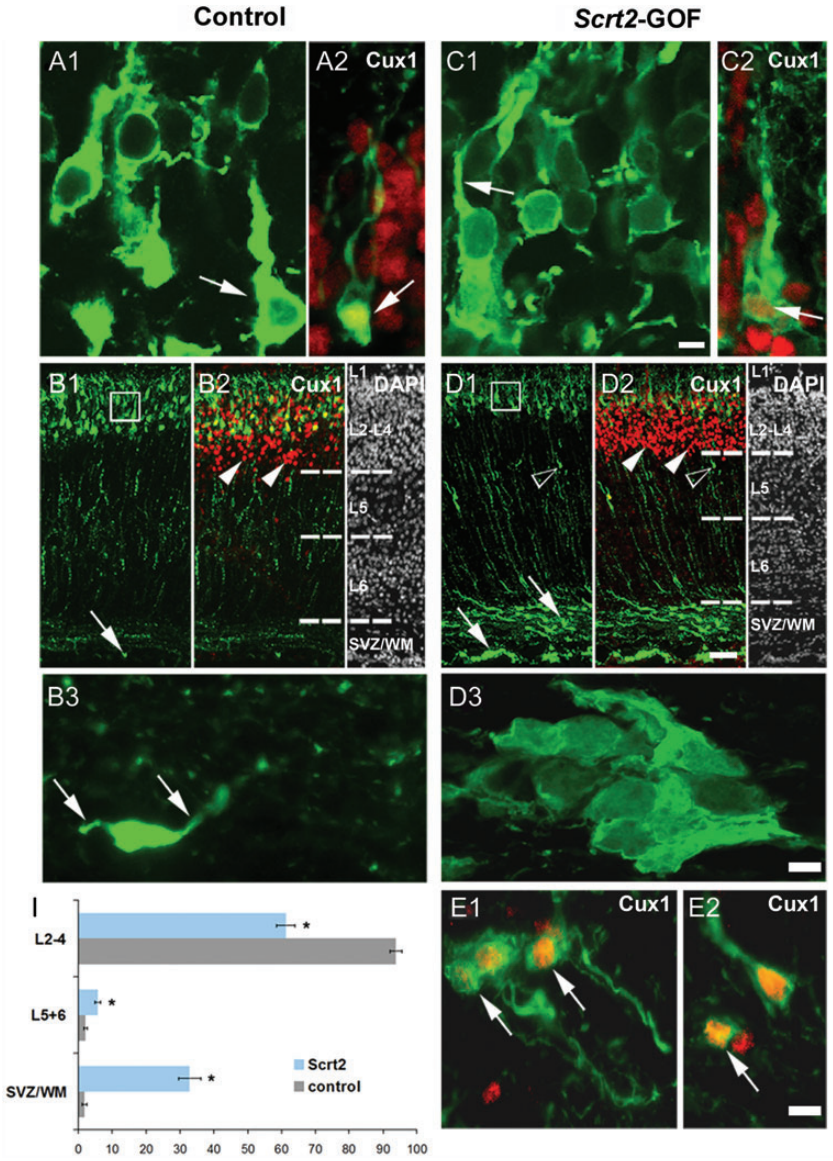

Figure 7. Migration defects in postnatal cortex upon forced expression of *Scrt2* in E14.5 embryonic brain. Embryo brains at E14.5 were electroporated by IUE and analyzed at P2. (*A1–B2*) Most of the CP neurons, descendants of progenitors electroporated with a control GFP vector, showed a pyramidal morphology (arrow in *A1*). They were positioned in the upper part of the expression domain of Cux1, a marker of L2–L4, but not in the deeper Cux1+ zone (L4, arrowheads in *B2*). Only few GFP+ cells were seen in the SVZ and subcortical white matter (WM) (arrow in *B1*), which appeared with a bipolar morphology (*B3*), characteristic of radially migrating neurons. (*C1–D2*) After IUE with *Scrt2-GFP* expression vector, much less GFP+ neurons succeeded to migrate into the CP delineated by the endogenous expression of Cux1 (white arrowheads in *D2*), and some GFP +/Cux1+ cells were spread in the deep cortical layers (*L6* and *L5*) (black arrowhead in *D1*, *D2*). (*B3–E2*) In contrast to the control, aggregates of multipolar GFP+ cells in the SVZ/WM (arrows in *D1*) were detected. Most of the trapped cells showed an immunostaining for Cux1 (*E1*,*E2*; also Supplementary Fig. 3*B1*,*B2*; *C*). (*I*) Statistical evaluation of the percentage of GFP+ cells (out of total GFP+ cells) localized in the indicated cortical zones at P2, $^*P < 0.05$. For all panels, GFP is visualized in green color, while respective markers—in red color. The images in *A1* and *C1* correspond to the frames in *B1* and *D1*, respectively. *D3*, *E1*, *E2* correspond to the region depicted by arrows in *D1*. Bars: 5 μm (*A1*, *A2*, *C1*, *C2*, *E1*, *E2*), 10 μm (*B3* and *D3*), 50 μm (*B1*,*B2*, *D1*,*D2*).

Supplementary Fig. 7). Moreover, 24 h after the electroporation, BrdU pulse labeling of cortical progenitors at E14.5 for 24 h showed a higher GFP+/BrdU+ ratio in *Scrt2KD* cortex when compared with the control, suggesting that a normal level of Scrt2 expression in SVZ/IZ supports the balance between proliferative and neurogenic IP divisions. Similar to the migrational defect observed after *Scrt2* overexpression that leads to the depletion of *Rnd2* expression (Fig. 8), *Scrt2KD* caused accumulation of shRNA-Scrt2-elctroporated cells in the SVZ/IZ of E15.5 cortex, most probably due to the reported retarded cell migration upon both diminishing or elevation of Rnd2 expression level (Heng et al. 2008).

Forced Expression in Cortical Progenitors Causes Defects in Radial Migration of the Generated Neurons

TFs of the Snail family have been demonstrated to influence cell migration (Barrallo-Gimeno and Nieto 2005). As noticed above, upon Scrt2GOF in transgenic mice, we also found evidence suggesting a migration problem of differentiated neurons toward the CP (Fig. 5*E*,*F*,*I–L*). We therefore used the

approach of forced focal overexpression in cortical progenitors through IUE to gain insights on the ability of *Scrt2* to control neuronal migration. IUEs were performed in E13.5 embryonic brains using *Scrt2* (*CMV-Scrt2-GFP*) or control vector (*CMV-GFP*). Three days after the electroporation, almost all of the GFP+ cells in the control brains left the proliferative zones and were located in the CP. In contrast, there was a massive accumulation of Scrt2-electroporated cells in the VZ/SVZ, where they showed exclusively multipolar morphology (data not shown).

To study if the phenotype reflects only a transitory migratory delay, the embryonic brains were electroporated at E14.5 and analyzed at P2 (Fig. 7). As specification of Cux1+ L4-L2 neurons initiates at stage E11.5, the endogenous

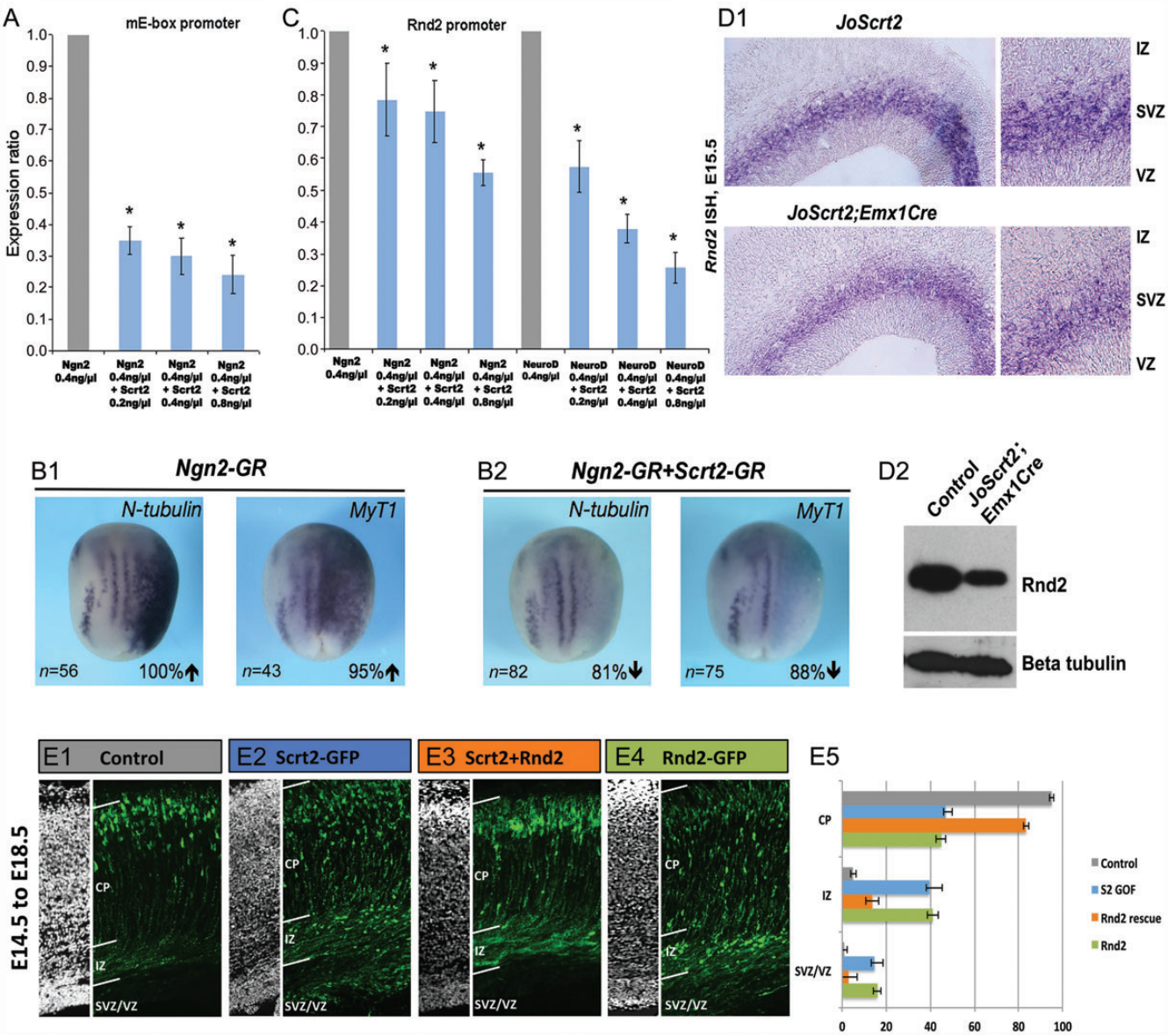

Figure 8. Scrt2 protein modifies the transcriptional activation of bHLH protein target genes. (*A*) P19 cells (cultured in 24 well plate) were transfected with a constant amounts multimerized luciferase-reporter construct (mEbox-Luc, 0.2 ng/µL) and Ngn2 activating expression construct *Ngn2*-pCS2 (0.4 ng/µL) together with increasing quantities (0.2, 0.4, and 0.8 ng/µL) of *Scrt2* expression plasmids. The luciferase activity was assayed after 24 h. The histograms represent values of 3 experiments (*Scrt2GOF*/control ratios, mean ± SEM). (*B1* and *B2*) Activation of *Scrt2-GR* inhibits the activity of Ngn2-GR on downstream targets in *Xenopus* embryos. *Ngn2-GR* mRNA alone (*B1*) or together with *Scrt2-GR* mRNA (*B2*) was injected and analyzed as described in Figure 2*A*. (*C*) P19 cells were transfected with *Rnd2* 3′ enhancer-Luc reporter (0.2 ng/µL) with either *Ngn2*-pCS2 or *NeuroD1*-pCS2 expression constructs (Heng et al. 2008) together with increasing quantities of either *Scrt2* expression vector, and assayed for luciferase activity after 24 h. The histograms represent values of 3 experiments (*Scrt2GOF*/control ratios, mean ± SEM). (*D1*) Decreased *Rnd2* expression in the mutant *Scrt2*; *Emx1Cre* cortex at E15.5, revealed by ISH on cross sections from embryonic control (*JoSCrt2* and transgenic (*JoScrt2*; *Emx1Cre*) (*D2*) Western blot analysis at E14.5 of cortical lysates revealed approximately 2.5-fold decreased level of Rnd2 protein in the transgenic when compared with control brains. (*E1–E4*) Simultaneous forced expression of *Scrt2* together with *Rnd2* rescued the migrational phenotype under *Scrt2GOF*. Electroporation of embryo brains was performed at E14.5 with expression plasmids: *GFP* (control empty vector (*E1*), *Scrt2-GFP* expression vector (*E2*), Rnd2-GFP expression plasmid (E4), or a mix (1:1) of *Scrt2-GFP* and *Rnd2-GFP* (*E3*). The brains were isolated and analyzed at E18.5. The black-white images illustrate the DAPI staining of the electroporated cortices. (*E4*) Statistical evaluation of the percentage of GFP+ cells (out of the total GFP+ cells) localized in the indicated zones. Values are presented as means ± SEM; $n = 4$ for *Scrt2.2-GOF* and rescue experiment, and $n = 3$ for GFP control; ($P < 0.05$). Bars: 100 µm (*D*), 50 µm (*E1–E3*).

expression of Cux1 in CP allows determination of the intracortical position of the GFP+ migrated cells (Zimmer et al. 2004). Even after such a prolonged period (6 days) following *Scrt2* overexpression, only a few GFP+ cells successfully reached the CP (Fig. 7*D1/B1*). The majority of the Scrt2-GFP+ cells showed multipolar morphology, being trapped in the SVZ/white matter (WM; Fig. 7*D2/B2*) and were negative for proliferative markers (Ki67, pH3, Tbr2, and Pax6, data not shown). Interestingly, IHC with Cux1 and Brn2, markers for UL neuronal fates, revealed a specific trapping of Cux1+ UL neurons in *Scrt2.2GOF* hemispheres, but not of Ctip2+ L5 neurons (Supplementary Fig. 8*A1/A2*). In accordance with IHC data with Smi-32 antibody at P10 (Fig. 3*E1*,*E2*), the pyramidal neurons in CP of the *Scrt2GOF* cortex were smaller and malformed when compared with the control CP (Fig. 7*C1/A1*,*C2/A2*). IHC with a Nestin antibody on E18.5 cortices, electroporated at E14.5, did not show any abnormalities of the RG cell processes (Supplementary Fig. 8*D1*–*D4*), suggesting that Scrt2 exerts a direct control on neuronal migration.

Scrt2 Competes with bHLH TF Ngn2 for E-box-Dependent Promoter Activation

To exert their activity, the proneuronal bHLH proteins interact and form heterodimers with ubiquitously expressed bHLH proteins (E12 and E47). This heteromeric complex then influences gene expression through binding to E-box motifs (CANNTG) within regulatory regions of target genes (Massari and Murre 2000). Similar to other Snail family members, all *Scratch* variants (human, murine, *Drosophila*, and *C. elegans*) also recognize and bind E-box motifs. As the proneural Neurogenins control cortical neurogenesis (Nieto 2001; Schuurmans et al. 2004) and neuronal migration (Hand et al. 2005; Ge et al. 2006; Heng et al. 2008; Pacary et al. 2011), we sought to determine if a competition exists between Scrt2 and Ngn2 for common DNA-binding targets by performing dual Luciferase-reporter assays in cultured P19 embryonic carcinoma cells. The cells were transfected with a multimerized *E-box* (*mE-box*) luciferase-reporter plasmid (0.2 ng/µL) together with a constant amount (0.4 ng/µL) of Ngn2 expression plasmid (Heng et al. 2008), and increasing amounts of Scrt2 expression plasmid (0.2, 0.4, and 0.8 ng/µL). Reporter activity was measured in cell lysates 24 h after transfection (efficiency >80%). Notably, the concentration dynamic profile with increasing amounts of Scrt2 expression vector caused a progressive repression (up to 46%) of the induction of the *E-box* reporter by the TF Ngn2 alone (thus when tested in the absence of Scratch2; Fig. 8*A*). Thus, similarly to what was shown for the human Scratch1 homolog, the mouse Scratch2 also has the ability to transcriptionally repress E-box motifs in reporter assay in vitro (Nakakura et al. 2001).

The results of the reporter assays suggest that Scrt2 protein may transrepress the Ngn2-dependent activation of E-box containing target genes in vivo. If indeed so, one would expect that, upon overexpression of *Scrt2*, Ngn2 target genes would be down-regulated. We first tested this possibility in the *Xenopus* system using whole-mount ISH expression analyses following single *Ngn2-GR* overexpression or coexpression with murine *Scrt2-GR* mRNA. While overexpression of *Ngn2-GR* mRNA strongly activated its direct downstream target gene *MyT1* (Bellefroid et al. 1996; Seo et al. 2007) as well as promoted strong ectopic neurogenesis as marked by *N-tubulin* (Ma et al. 1996; Perron et al. 1999), coinjection with *Scrt2-GR* mRNA abolished the ability of Ngn2 to activate these genes (Fig. 8*B1*,*B2*). In contrast, coinjection of *GFP* mRNA together with *Ngn2* mRNA did not disrupt the ability of Ngn2 to promote neurogenesis (Supplementary Fig. 5). Taken together, these findings suggest that, in vertebrates, Scrt2 influences the expression of bHLH downstream target genes via a competition for E-box containing common targets.

Rnd2 Coexpression Rescues the Migrational Defect Upon Focal Scrt2 Overexpression in the Developing Cortex

Ngn2 directly activates *Rnd2*, which encodes for a small GTP-binding protein that plays an essential role for the transition from multipolar to bipolar state of the migrating neurons in the SVZ/IZ (Nakamura et al. 2006; Heng et al. 2008). Given the demonstrated capacity of Scrt2 to compete with Ngn2 for common *E-box* containing targets sites, as well as the colocalization of Scrt2 with Ngn2 in a subset of progenitors in the VZ/SVZ (Fig. 2*D1*–*D4*) and with NeuroD1+ in differentiating neurons at the SVZ/IZ border (Fig. 1*B1*), we speculated that a competition between Scrt2 with these 2 bHLH factors may modulate the locomotion of the neurons through a direct influence on *Rnd2* expression and activity. To directly examine this possibility, we first analyzed the influence of Scrt2 on the transcriptional regulation of a luciferase-reporter plasmid containing the *Rnd2* 3′ enhancer (Heng et al. 2008). As shown by Heng et al. (2008), the identified *Rnd2 3′* enhancer is directly activated by Ngn2 or NeuroD1, which are sequentially expressed in the VZ and IZ/CP, respectively. Indeed, the coexpression of constant amounts of the activators, either Ngn2 or NeuroD1, with increasing amounts of Scrt2 expression plasmid, led to a profound transrepression of the *Rnd2*-reporter activity (up to 44.4% of the Ngn2 activity alone and up to 74.3% of the NeuroD1 activity, Fig. 8*C*). In agreement with the endogenous colocalization of Scrt2 with Ngn2 and NeuroD1 in subsets of cells in the VZ or SVZ/IZ, respectively, *Scrt2* overexpression in vivo led to a mild decrease of *Rnd2* expression in the *JoScrt2*; *Emx1Cre* embryo cortex detected by ISH and western blot analyses at stage E14.5–E15.5, respectively (Fig. 8*D1*,*D2*). Together, these findings suggest that Scrt2 acts as a transrepressor, fine-tuning *Rnd2* expression.

As suppression of *Rnd2* expression in cortical progenitors affects the locomotion of the neurons toward the CP (Heng et al. 2008), it was tempting to examine if reconstitution of the Rnd2 level upon *Scrt2GOF* could rescue the observed migration defect. To examine this possibility, we performed IUEs of E14.5 embryo brains either with a control empty vector (pCIG2-GFP), Scrt2-GFP expression vector alone, or together with Rnd2-GFP expression vector. Four days following electroporation, almost all of the electroporated GFP+ cells in the control cortex have migrated from the VZ/SVZ across the IZ ($5 \pm 1.35\%$, $n = 3$, $P < 0.05$) and already reached the uppermost region of the CP ($95 \pm 1.34\%$, $n = 3$, $P < 0.05$; Fig. 8*E1*, *E5*). In contrast, electroporation with CMV-Scrt2 vector disturbed the migration of these cells, which accumulated in the SVZ ($14.7 \pm 3.2\%$, $n = 4$, $P < 0.05$) and in the IZ ($39.5 \pm 5.7\%$, $n = 4$, $P < 0.05$) Those cells that reached the CP were mostly found in the deeper part of the CP ($46.7 \pm 3.76\%$, $n = 4$,

$P < 0.05$; Fig. 8*E*2,*E*5). In agreement with the data of Heng et al. (2008), Rnd2 overexpression alone also exerted a mild migratory phenotype (Fig. 8*E*4). In contrast to the massive cell accumulation observed in the IZ of the *Scrt2GOF* cortex, in the rescue experiment, most cells detached and migrated successfully into the upper CP (83.4 ± 4%, $n = 4$, $P < 0.05$; Fig. 8*E*3,*E*5) and only a small percentage were retained in the IZ (13.7 ± 1.35%, $n = 4$, $P < 0.05$).

Altogether, these findings suggest that, through antagonism of the bHLH-dependent transcriptional regulation of *Rnd2*, Scrt2 modulates the ability of neurons generated in germinative zones to migrate radially toward the cortex.

Discussion

In vertebrates, the *Snail* genes are subdivided into 3 *Snail* (*Snail1*, *2*, and *3*) and 2 *Scratch* (*Scrt1*, *Scr2*) family members (Barrallo-Gimeno and Nieto 2009). While *Snail* members have been demonstrated to play essential roles during mesoderm and neural crest formation, melanocyte development, spermatogenesis, and tumorigenesis (Nieto et al. 1994; Come et al. 2004; Barrallo-Gimeno and Nieto 2005; Peinado et al. 2005; Cobaleda et al. 2007; Bastid et al. 2010), the function of *Scrt* members in vertebrates, especially of *Scrt2*, is unknown. Here, we present evidence that Scrt2 modulates cortical neurogenesis and neuronal migration in mammals.

Scrt2 Influences the Choice for the Direct Versus Indirect Mode of Cortical Neurogenesis

The present study supports and further extends previous expression data from ISH analysis, demonstrating expression of *Scrt2* in differentiating and migrating neurons in the developing mouse cortex (Marin and Nieto 2006). In addition, IHC analysis revealed expression of Scrt2 in a subset of apically dividing RGPs as well as proliferating and neurogenic Insm1+ IPs. The immunostaining with anti-Scrt2 antibody revealed punctuate nuclear and or more homogeneous cytoplasmic expression in cortical progenitors at the apical VZ surface. In different cell lines, Snail proteins were detected predominantly either in the nucleus, cytosol, or in both compartments, suggesting that functions of Snail family members are controlled by subcellular localization (Dominguez et al. 2003; Yamasaki et al. 2005). While the N-terminal half of the Snail and Scratch proteins are divergent, the C-terminal 6 ZFs that mediate DNA binding are highly conserved (Mingot et al. 2009). For efficient transport into the nucleus, Snail proteins rely on interaction of the nuclear location signal (a highly conserved basic residues in at least 3 consecutive ZFs), with distinct Importins (Yamasaki et al. 2005; Mingot et al. 2009). In their ZFs, the Scratch proteins have only 2 conserved basic residues and possible partners for Scratch nuclear import are still unknown. However, proteins <40 kDa are able to pass through nuclear pore complexes by passive diffusion (Görlich and Kutay 1999), and the presence of one (in Wt1, Bruening et al. 1996) or even a half ZF (in GKLF 9, Shields et al. 1996) was sufficient for nuclear migration, suggesting that Scratch2 (33 kDa) would have the capacity to translocate into the nucleus and acts as a TF. Indeed, following forced in vivo overexpression of Scrt2 in cortical progenitors, the cells trapped in the SVZ showed a clear nuclear expression of Scrt2, while, after differentiation and migration, the Scrt2 expression in the CP GFP+ neurons was mostly cytoplasmic. As recently demonstrated by Zhang et al. (2012), epithelial-to-mesenchymal transitions in the developing embryo are critically dependent on the subcellular (nuclear/cytoplasmic) location of the Snail1 protein. In the nucleus, phosphorylation of Snail1 by Lat2 kinase is essential for subsequent post-translational modifications underlying Snail1 protein stability and function as a TF (Zhang et al. 2012). Therefore, elucidation of the mechanism regulating Scrt2 subcellular localization is an important topic for a further investigation.

We found that Scrt2 is expressed in the VZ in subsets of dividing Pax6+ RGPs or neurogenic Insm1+ IPs, as well as in Tbr2+ IPs and differentiating/nascent neurons located in the upper SVZ and SVZ/IZ border. RGPs in the VZ show apical-basal polarity with apical localization of a number of signaling cues that regulates RGP proliferation and/or adhesion (Rakic 1972, 2003; Huang and He 2008; Bultje et al. 2009). Moreover, recent evidence indicate that, localized to centrosome of neuronal progenitors, β-catenin plays an essential role in the maintenance of neural progenitor polarity and the regulation of neurogenic cell cycle exit (Chilov et al. 2011). Upon a mild in vivo conditional overexpression of *Scrt2* at the onset of neurogenesis (reaching up to a 2-fold increase over the normal in vivo level), we found that, in the frame of 1 mitotic cycle (E12.5–E13.5), the progenitors proliferation and exit from mitosis appeared unaltered, but they showed preferable generation of Tbr1+ neurons, instead of Tbr2+ cells. In agreement with these findings, quantitative results from our clonal pair-cell analysis after in vivo forced expression of Scrt2 through IUE clearly showed an excess of neurons generated via direct neurogenesis. On the contrary, in vivo KD of Scrt2 in E13.5 embryo brain led to an enhancement of the generation of Tbr2+ cells. Altogether, these results suggest that, at early stages of cortical development, Scrt2GOF in vivo favors progenitor neurogenic (P → P + N) over the progenitor proliferative (P → P + IP) asymmetric division.

Despite the temporary increase of early neurogenesis at E12.5, due to the decreased production of IPs, the final neuronal output for the mature CP was reduced, leading to only a moderate thinning of the mature caudal cortex, and depletion of the generated upper neuronal subtypes as seen at P10 in the *Scrt2GOF* cortex. The region-specific phenotype upon conditional overexpression of *Scrt2* seems to reflects the previously reported caudomedial high to rostrolateral low early activation of Cre-recombinase activity by the *Emx1Cre* line (Li et al. 2003), which, in fact, parallels the endogenous expression gradient of *Scrt2* (this study), leading to a more prominent overexpression phenotype in the caudomedial pallium. Noteworthy, a mild phenotype appears to be a common feature upon manipulation of the *Scratch* expression level, reported for the *Drosophila* pan-neuronal *scratch* (1 of the 3 so far known fly *scratch-like1* and *scratch-like2* genes; Roark et al. 1995), suggesting a limited penetrance of the individual phenotype of a particular *Scratch* gene that was also shown for the *Drosophila Snail* genes (Ashraf et al. 2009).

Interestingly, despite the unique features of neurogenesis in the mammalian cortex as opposed to other vertebrates including "amphibians", the final outcome upon *Scrt2GOF* in both transgenic mice and *Xenopus* embryos was similar, namely a profound inhibition of the primary neurogenesis in *Xenopus laevis*, and selective inhibition of the indirect mode

of neurogenesis mediated by IPs in the developing mammalian neocortex. The finding that Scrt2GOF forces neuronal differentiation are in general agreement with the reported effect for the mouse *Scratch* gene in P19 embryonal carcinoma cells (Nakakura et al. 2001), as well as with the strong increase of Scrt2 expression level in the forebrain of the zebrafish "mind bomb" mutant in which a profound premature neuronal differentiation occurs (Dam et al. 2011). The enforced acquisition of neuronal fate therefore appears to be a common feature of Scratch proteins as reported in GOF assays for *Drosophila Scratch1* (Emery and Bier 1995; Roark et al. 1995; Seugnet et al. 1997) and *C. elegans* ortholog, *ces-1* (Ellis and Horvitz 1991).

Scrt2 Modulates the Rnd2-Dependent Locomotion of Cortical Neurons

Born in the germinative zones, neurons with monopolar or bipolar morphology undertake long journeys toward the CP, using 2 migrational modes, locomotion, and somal translocation, respectively (Rakic 1972; Miyata et al. 2001; Nadarajah et al. 2003). The generated neurons detach from the VZ, acquire a multipolar shape, and when they reach the SVZ, pause for a certain time (Bayer et al. 1991) before retransforming to a bipolar shape for their radial migration along the RG cell processes toward CP. After reaching the lower zone of CP at perinatal stages, the locomoting immature neurons pause and then invade the outermost zone of the CP using again a translocation (Sekine et al. 2011). A third mode of cell migration, named "multipolar migration", has been described for a subpopulation of postmitotic neurons that accumulate at the SVZ/IZ border (Tabata and Nakajima 2003). Such multipolar cells do not move directly toward the CP, but instead they take a tangential migration (Sasaki et al. 2008) in the SVZ/IZ before undergoing radial migration.

Here, we show that forced overexpression of Scrt2 in cortical progenitors results in a robust accumulation of cells with multipolar shape in the SVZ or SVZ/IZ border, where the endogenous *Scrt2* is strongly expressed. This finding implicates a role for Scrt2 in keeping freshly born neurons in these "sojourn zones" (Altman and Bayer 1990) before initiating their radial migration toward the CP. Upon forced in vivo overexpression of *Scrt2* at E14.5, a substantial portion of the Scrt2 overexpressing cells was hampered in their ability to detach from SVZ/IZ and undertake locomotion, even at P2. However, despite their altered morphology, the accumulated cells displayed the correct temporal fate and differentiated into Cux1+ UL neurons.

Through the coordination of neurogenesis and neuronal migration, proneural bHLH proteins play crucial roles during cortical neurogenesis (Bertrand et al. 2002; Guillemot et al. 2006), including promotion of progenitor mitosis at the basal VZ surface, IP maturation in the SVZ, and neuronal migration (Miyata et al. 2004; Britz et al. 2006). Our results strongly suggest that Scrt2 is a coregulator of bHLH-dependent neuronal motility. Migrational defects similar to those observed upon *Scrt2GOF* have also been observed in *Ngn2/1KO* mice (Schuurmans et al. 2004; Hand et al. 2005) and upon silencing of the Ngn2 target gene *Rnd2* (Heng et al. 2008). The small Rnd family of atypical Rho GTPases consists of 2 members, Rnd2 and Rnd3 (Chardin 2006). These proteins have the capacity to inhibit RhoA signaling, thereby promoting neuronal migration (Ge et al. 2006; Pacary et al. 2011). Notably, both Scrt2 and Rnd2 are expressed in a subset of Ngn2+ RGPs in the VZ, but not in Tbr2+ progenitors in the VZ/lower SVZ (this study Fig. 1, Heng et al. 2008). In P19 cells, Scrt2 inhibited, in a dose-dependent manner, the Ngn2- or NeuroD1-mediated activation of an *Rnd2*-enhancer reporter construct (Fig. 8*C*). This suggests that the defects in neuronal migration observed upon forced expression of Scrt2 in vivo might be due to competition between Scrt2 and the bHLH TF Ngn2 and NeuroD1 in the VZ/SVZ and IZ, respectively, for the activation of *Rnd2*. Indeed, in the *Scrt2GOF* cortex at E15.5, the ISH (Fig. 8*D*1) and western blot analysis (Fig. 8*D*2) demonstrated an inhibition of Rnd2 expression in the mutant cortex at both the transcriptional and protein level. Moreover, in an in vivo rescue experiment, we found that the migratory deficiency of the neurons upon *Scrt2GOF* was almost fully compensated through the simultaneous coexpression of *Rnd2*. In addition to a migrational defect, overexpression of Scrt2 also altered the morphology of the Smi-32+ pyramidal L5 neurons, with a significantly diminished size of their soma in the *JoScrt2*; *Emx1Cre* postnatal cortex observed. Neuronal migration involves reorganization of the cytoskeleton in which the RhoGTPases play crucial roles (Marin et al. 2006; Heasman and Ridley 2008). Similarly to the reported cellular localization of Rnd2 expression (Heng et al. 2008), Scrt2 was predominantly expressed in the soma of Tbr2+ and NeuroD1 + IPs/newly born neurons in the upper SVZ/IZ, implicating the functional interaction between the 2 factors in neuronal soma in controlling neuronal migration.

Although IPs are assumed to play a unique role in the generation of the primate neocortex, characterized by a huge expansion of the upper neuronal layers that form folds and grooves (Smart et al. 2002; Rakic 2003; 2009; Kriegstein et al. 2006; Molnar et al. 2006; Bystron et al. 2008), the molecular mechanisms underlying the IP genesis are not sufficiently understood. The results presented in this study demonstrate that the mammalian TF Scrt2 modulates neurogenesis and neuronal migration in the developing cortex through competition with bHLH-TFs for common gene targets regulatory elements. In light of the recently identified proneural gene regulatory network (Gohlke et al. 2008), it will be of interest in the future to analyze the specific molecular interaction between bHLH proteins with Scratch proteins and the consequence for the fine-tuning of neurogenesis in the developing mammalian brain.

Supplementary Material

Supplementary material can be found at: http://www.cercor.oxfordjournals.org/.

Funding

This work was supported by the Max-Planck Gesellschaft (A.S., V.P., and E.P.) and Cluster of Excellence Nanoscale Microscopy and Molecular Physiology of the Brain, CNMPB, (V.P., A.S., B. R., K.H., and T.P.). A.B.T. was supported by a fellowship from the Alexander von Humboldt Foundation (www.avh.de).

Notes

We thank M. Daniel, S. Schlott, and K. Ditter for excellent technical assistance.

We are grateful to F. Guillemot (London, UK) for providing the expression plasmids *pCS2-Ngn2*, *pCS2-NeuroD1*, *CMV- Rnd2*, the *Rnd2-3′-Luc* reporter vector, and the plasmid for generation of *Rnd2* and *Ngn2* in situ probes. We thank David J. Anderson, (California Institute of Technology, CA, USA) and Carmen Birchmeier-Kohler, (Max-Delbrück-Center for Molecular Medicine, Berlin, Germany) for the provision of the anti-Ngn2 and anti-Insm1 antibodies, and J. Liu (Beth Israel Deaconess Medical Center, Bosten, MA, USA) for the *Cux2* in situ probe template. *Conflict of Interest*: None declared.

References

Alcamo EA, Chirivella L, Dautzenberg M, Dobreva G, Farinas I, Grosschedl R, McConnell SK. 2008. Satb2 regulates callosal projection neuron identity in the developing cerebral cortex. Neuron. 57:364–377.

Altman J, Bayer SA. 1990. Prolonged sojourn of developing pyramidal cells in the intermediate zone of the hippocampus and their settling in the stratum pyramidale. J Comp Neurol. 301:343–364.

Anthony TE, Klein C, Fishell G, Heintz N. 2004. Radial glia serve as neuronal progenitors in all regions of the central nervous system. Neuron. 41:881–890.

Arlotta P, Molyneaux BJ, Chen J, Inoue J, Kominami R, Macklis JD. 2005. Neuronal subtype-specific genes that control corticospinal motor neuron development in vivo. Neuron. 45:207–221.

Armentano M, Chou SJ, Tomassy GS, Leingartner A, O'Leary DD, Studer M. 2007. COUP-TFI regulates the balance of cortical patterning between frontal/motor and sensory areas. Nat Neurosci. 10:1277–1286.

Arnold SJ, Huang GJ, Cheung AF, Era T, Nishikawa S, Bikoff EK, Molnar Z, Robertson EJ, Groszer M. 2008. The T-box transcription factor Eomes/Tbr2 regulates neurogenesis in the cortical subventricular zone. Genes Dev. 22:2479–2484.

Ashraf SI, Hu X, Roote J, Ip YT. 2009. The mesoderm determinant snail collaborates with related zinc-finger proteins to control *Drosophila* neurogenesis. EMBO J. 18:983–992.

Barrallo-Gimeno A, Nieto MA. 2005. The Snail genes as inducers of cell movement and survival: implications in development and cancer. Development. 132:3151–3161.

Barrallo-Gimeno A, Nieto MA. 2009. Evolutionary history of the Snail/Scratch superfamily. Trends Genet. 25:248–252.

Bastid J, Bouchet BP, Ciancia C, Pourchet J, Audoynaud C, Grelier G, Puisieux A, Ansieau S. 2010. The SNAIL family member SCRATCH1 is not expressed in human tumors. Oncol Rep. 23:523–529.

Bayer SA, Altman J, Russo RJ, Dai XF, Simmons JA. 1991. Cell migration in the rat embryonic neocortex. J Comp Neurol. 307:499–516.

Bellefroid EJ, Bourguignon C, Hollemann T, Ma Q, Anderson DJ, Kintner C, Pieler T. 1996. X-MyT1, a Xenopus C2HC-type zinc finger protein with a regulatory function in neuronal differentiation. Cell. 87:1191–1202.

Berger J, Berger S, Tuoc TC, D'Amelio M, Cecconi F, Gorski JA, Jones KR, Gruss P, Stoykova A. 2007. Conditional activation of Pax6 in the developing cortex of transgenic mice causes progenitor apoptosis. Development. 134:1311–1322.

Bertrand N, Castro DS, Guillemot F. 2002. Proneural genes and the specification of neural cell types. Nat Rev Neurosci. 3:517–530.

Borello U, Pierani A. 2010. Patterning the cerebral cortex: traveling with morphogens. Curr Opin Genet Dev. 20:408–415.

Britanova O, de Juan Romero C, Cheung A, Kwan KY, Schwark M, Gyorgy A, Vogel T, Akopov S, Mitkovski M, Agoston D et al. 2008. Satb2 is a postmitotic determinant for upper-layer neuron specification in the neocortex. Neuron. 57:378–392.

Britz O, Mattar P, Nguyen L, Langevin LM, Zimmer C, Alam S, Guillemot F, Schuurmans C. 2006. A role for proneural genes in the maturation of cortical progenitor cells. Cereb Cortex. 16 (Suppl 1): i138–i151.

Bruening W, Moffett P, Chia S, Heinrich G, Pelletier J. 1996. Identification of nuclear localization signals within the zinc fingers of the WT1 tumor suppressor gene product. FEBS Lett. 393:41–47.

Bultje RS, Castaneda-Castellanos DR, Jan LY, Jan YN, Kriegstein AR, Shi SH. 2009. Mammalian Par3 regulates progenitor cell asymmetric division via notch signaling in the developing neocortex. Neuron. 63:189–202.

Bystron I, Blakemore C, Rakic P. 2008. Development of the human cerebral cortex: Boulder Committee revisited. Nat Rev Neurosci. 9:110–122.

Cappello S, Attardo A, Wu X, Iwasato T, Itohara S, Wilsch-Brauninger M, Eilken HM, Rieger MA, Schroeder TT, Huttner WB et al. 2006. The Rho-GTPase cdc42 regulates neural progenitor fate at the apical surface. Nat Neurosci. 9:1099–1107.

Caviness VS Jr, Takahashi T. 1995. Proliferative events in the cerebral ventricular zone. Brain Dev. 17:159–163.

Chardin P. 2006. Function and regulation of Rnd proteins. Nat Rev Mol Cell Biol. 7:54–62.

Chilov D, Sinjuashina N, Rita H, Taketo MM, Mäkelä TP, Partanen J. 2011. Phosphorylated β-catenin localizes to centrosomes of neuronal progenitors and is required for cell polarity and neurogenesis in developing midbrain. Dev Biol. 357:259–268.

Chitnis AB. 1995. The role of Notch in lateral inhibition and cell fate specification. Mol Cell Neurosci. 6:311–321.

Cho JH, Tsai MJ. 2004. The role of BETA2/NeuroD1 in the development of the nervous system. Mol Neurobiol. 30:35–47.

Cobaleda C, Perez-Caro M, Vicente-Duenas C, Sanchez-Garcia I. 2007. Function of the zinc-finger transcription factor SNAI2 in cancer and development. Annu Rev Genet. 41:41–61.

Come C, Arnoux V, Bibeau F, Savagner P. 2004. Roles of the transcription factors snail and slug during mammary morphogenesis and breast carcinoma progression. J Mammary Gland Biol Neoplasia. 9:183–193.

Cubelos B, Sebastian-Serrano A, Kim S, Moreno-Ortiz C, Redondo JM, Walsh CA, Nieto M. 2008. Cux-2 controls the proliferation of neuronal intermediate precursors of the cortical subventricular zone. Cereb Cortex. 18:1758–1770.

Dam TM, Kim HT, Moon HY, Hwang KS, Jeong YM, You KH, Lee JS, Kim CH. 2011. Neuron-specific expression of Scratch genes during early zebrafish development. Mol Cells. 31:471–475.

Dominguez D, Montserrat-Sentis B, Virgos-Soler A, Guaita S, Grueso J, Porta M, Puig I, Baulida J, Franci C, Garcia de Herreros A. 2003. Phosphorylation regulates the subcellular location and activity of the snail transcriptional repressor. Mol Cell Biol. 23:5078–5089.

Ellis RE, Horvitz HR. 1991. Two C. elegans genes control the programmed deaths of specific cells in the pharynx. Development. 112:591–603.

Emery JF, Bier E. 1995. Specificity of CNS and PNS regulatory subelements comprising pan-neural enhancers of the deadpan and scratch genes is achieved by repression. Development. 121:3549–3560.

Englund C, Fink A, Lau C, Pham D, Daza RA, Bulfone A, Kowalczyk T, Hevner RF. 2005. Pax6, Tbr2, and Tbr1 are expressed sequentially by radial glia, intermediate progenitor cells, and postmitotic neurons in developing neocortex. J Neurosci. 25:247–251.

Farkas LM, Haffner C, Giger T, Khaitovich P, Nowick K, Birchmeier C, Paabo S, Huttner WB. 2008. Insulinoma-associated 1 has a panneurogenic role and promotes the generation and expansion of basal progenitors in the developing mouse neocortex. Neuron. 60:40–55.

Gammill LS, Sive H. 1997. Identification of otx2 target genes and restrictions in ectodermal competence during Xenopus cement gland formation. Development. 124:471–481.

Ge W, He F, Kim KJ, Blanchi B, Coskun V, Nguyen L, Wu X, Zhao J, Heng JI, Martinowich K et al. 2006. Coupling of cell migration with neurogenesis by proneural bHLH factors. Proc Natl Acad Sci USA. 103:1319–1324.

Gohlke JM, Armant O, Parham FM, Smith MV, Zimmer C, Castro DS, Nguyen L, Parker JS, Gradwohl G, Portier CJ et al. 2008. Characterization of the proneural gene regulatory network during mouse telencephalon development. BMC Biol. 6:15.

Görlich D, Kutay U. 1999. Transport between the cell nucleus and the cytoplasm. Annu Rev Cell Dev Biol. 15:607–660.
Gorski JA, Talley T, Qiu M, Puelles L, Rubenstein JL, Jones KR. 2002. Cortical excitatory neurons and glia, but not GABAergic neurons, are produced in the Emx1-expressing lineage. J Neurosci. 22:6309–6314.
Götz M, Huttner WB. 2005. The cell biology of neurogenesis. Nat Rev Mol Cell Biol. 6:777–788.
Götz M, Stoykova A, Gruss P. 1998. Pax6 controls radial glia differentiation in the cerebral cortex. Neuron. 21:1031–1044.
Grimes HL, Chan TO, Zweidler-McKay PA, Tong B, Tsichlis PN. 1996. The Gfi-1 proto-oncoprotein contains a novel transcriptional repressor domain, SNAG, and inhibits G1 arrest induced by interleukin-2 withdrawal. Mol Cell Biol. 16:6263–6272.
Guillemot F, Molnar Z, Tarabykin V, Stoykova A. 2006. Molecular mechanisms of cortical differentiation. Eur J Neurosci. 23:857–868.
Hand R, Bortone D, Mattar P, Nguyen L, Heng JI, Guerrier S, Boutt E, Peters E, Barnes AP, Parras C et al. 2005. Phosphorylation of Neurogenin2 specifies the migration properties and the dendritic morphology of pyramidal neurons in the neocortex. Neuron. 48:45–62.
Hardcastle Z, Papalopulu N. 2000. Distinct effects of XBF-1 in regulating the cell cycle inhibitor p27(XIC1) and imparting a neural fate. Development. 127:1303–1314.
Harland RM. 1991. In situ hybridization: an improved whole-mount method for Xenopus embryos. Methods Cell Biol. 36:685–695.
Haubensak W, Attardo A, Denk W, Huttner WB. 2004. Neurons arise in the basal neuroepithelium of the early mammalian telencephalon: a major site of neurogenesis. Proc Natl Acad Sci USA. 101:3196–3201.
Heasman SJ, Ridley AJ. 2008. Mammalian Rho GTPases: new insights into their functions from in vivo studies. Nat Rev Mol Cell Biol. 9:690–701.
Heins N, Malatesta P, Cecconi F, Nakafuku M, Tucker KL, Hack MA, Chapouton P, Barde YA, Gotz M. 2002. Glial cells generate neurons: the role of the transcription factor Pax6. Nat Neurosci. 5:308–315.
Hemavathy K, Ashraf SI, Ip YT. 2000. Snail/slug family of repressors: slowly going into the fast lane of development and cancer. Gene. 257:1–12.
Heng JI, Nguyen L, Castro DS, Zimmer C, Wildner H, Armant O, Skowronska-Krawczyk D, Bedogni F, Matter JM, Hevner R et al. 2008. Neurogenin 2 controls cortical neuron migration through regulation of Rnd2. Nature. 455:114–118.
Hevner RF, Daza RA, Rubenstein JL, Stunnenberg H, Olavarria JF, Englund C. 2003. Beyond laminar fate: toward a molecular classification of cortical projection/pyramidal neurons. Dev Neurosci. 25:139–151.
Hevner RF, Hodge RD, Daza RA, Englund C. 2006. Transcription factors in glutamatergic neurogenesis: conserved programs in neocortex, cerebellum, and adult hippocampus. Neurosci Res. 55:223–233.
Hevner RF, Shi L, Justice N, Hsueh Y, Sheng M, Smiga S, Bulfone A, Goffinet AM, Campagnoni AT, Rubenstein JL. 2001. Tbr1 regulates differentiation of the preplate and layer 6. Neuron. 29:353–366.
Hill RE, Favor J, Hogan BL, Ton CC, Saunders GF, Hanson IM, Prosser J, Jordan T, Hastie ND, van Heyningen V. 1991. Mouse small eye results from mutations in a paired-like homeobox-containing gene. Nature. 354:522–525.
Huang H, He X. 2008. Wnt/beta-catenin signaling: new (and old) players and new insights. Curr Opin Cell Biol. 20:119–125.
Klisch TJ, Souopgui J, Juergens K, Rust B, Pieler T, Henningfeld KA. 2006. Mxi1 is essential for neurogenesis in Xenopus and acts by bridging the pan-neural and proneural genes. Dev Biol. 292:470–485.
Kolm PJ, Sive HL. 1995. Efficient hormone-inducible protein function in Xenopus laevis. Dev Biol. 171:267–272.
Kowalczyk T, Pontious A, Englund C, Daza RA, Bedogni F, Hodge R, Attardo A, Bell C, Huttner WB, Hevner RF. 2009. Intermediate neuronal progenitors (basal progenitors) produce pyramidal-projection neurons for all layers of cerebral cortex. Cereb Cortex. 19:2439–2450.
Kriegstein A, Noctor S, Martinez-Cerdeno V. 2006. Patterns of neural stem and progenitor cell division may underlie evolutionary cortical expansion. Nat Rev Neurosci. 7:883–890.
Lamborghini JE. 1980. Rohon-beard cells and other large neurons in Xenopus embryos originate during gastrulation. J Comp Neurol. 189:323–333.
Li HS, Wang D, Shen Q, Schonemann MD, Gorski JA, Jones KR, Temple S, Jan LY, Jan YN. 2003. Inactivation of Numb and Numblike in embryonic dorsal forebrain impairs neurogenesis and disrupts cortical morphogenesis. Neuron. 40:1105–1118.
Ma Q, Kintner C, Anderson DJ. 1996. Identification of neurogenin, a vertebrate neuronal determination gene. Cell. 87:43–52.
Malatesta P, Appolloni I, Calzolari F. 2008. Radial glia and neural stem cells. Cell Tissue Res. 331:165–178.
Malatesta P, Hack MA, Hartfuss E, Kettenmann H, Klinkert W, Kirchhoff F, Gotz M. 2003. Neuronal or glial progeny: regional differences in radial glia fate. Neuron. 37:751–764.
Mallamaci A, Stoykova A. 2006. Gene networks controlling early cerebral cortex arealization. Eur J Neurosci. 23:847–856.
Marin F, Nieto MA. 2006. The expression of Scratch genes in the developing and adult brain. Dev Dyn. 235:2586–2591.
Marin O, Valdeolmillos M, Moya F. 2006. Neurons in motion: same principles for different shapes? Trends Neurosci. 29:655–661.
Massari ME, Murre C. 2000. Helix-loop-helix proteins: regulators of transcription in eucaryotic organisms. Mol Cell Biol. 20:429–440.
McConnell SK. 1991. The generation of neuronal diversity in the central nervous system. Ann Rev Neurosci. 14:269–300.
Metzstein MM, Horvitz HR. 1999. The C. elegans cell death specification gene ces-1 encodes a snail family zinc finger protein. Mol Cell. 4:309–319.
Mingot JM, Vega S, Maestro B, Sanz JM, Nieto MA. 2009. Characterization of Snail nuclear import pathways as representatives of C2H2 zinc finger transcription factors. J Cell Sci. 122:1452–1460.
Miyata T, Kawaguchi A, Okano H, Ogawa M. 2001. Asymmetric inheritance of radial glial fibers by cortical neurons. Neuron. 31:727–741.
Miyata T, Kawaguchi A, Saito K, Kawano M, Muto T, Ogawa M. 2004. Asymmetric production of surface-dividing and non-surface-dividing cortical progenitor cells. Development. 131:3133–3145.
Molnar Z, Metin C, Stoykova A, Tarabykin V, Price DJ, Francis F, Meyer G, Dehay C, Kennedy H. 2006. Comparative aspects of cerebral cortical development. Eur J Neurosci. 23:921–934.
Molyneaux BJ, Arlotta P, Hirata T, Hibi M, Macklis JD. 2005. Fezl is required for the birth and specification of corticospinal motor neurons. Neuron. 47:817–831.
Molyneaux BJ, Arlotta P, Menezes JR, Macklis JD. 2007. Neuronal subtype specification in the cerebral cortex. Nat Rev Neurosci. 8:427–437.
Mühlfriedel S, Kirsch F, Gruss P, Chowdhury K, Stoykova A. 2007. Novel genes differentially expressed in cortical regions during late neurogenesis. Eur J Neurosci. 26:33–50.
Nadarajah B, Alifragis P, Wong RO, Parnavelas JG. 2003. Neuronal migration in the developing cerebral cortex: observations based on real-time imaging. Cereb Cortex. 13:607–611.
Nakakura EK, Watkins DN, Schuebel KE, Sriuranpong V, Borges MW, Nelkin BD, Ball DW. 2001. Mammalian Scratch: a neural-specific Snail family transcriptional repressor. Proc Natl Acad Sci USA. 98:4010–4015.
Nakakura EK, Watkins DN, Sriuranpong V, Borges MW, Nelkin BD, Ball DW. 2001. Mammalian Scratch participates in neuronal differentiation in P19 embryonal carcinoma cells. Brain Res Mol Brain Res. 95:162–166.
Nakamura K, Yamashita Y, Tamamaki N, Katoh H, Kaneko T, Negishi M. 2006. In vivo function of Rnd2 in the development of neocortical pyramidal neurons. Neurosci Res. 54:149–153.
Nieto M, Monuki ES, Tang H, Imitola J, Haubst N, Khoury SJ, Cunningham J, Gotz M, Walsh CA. 2004. Expression of Cux-1 and

Cux-2 in the subventricular zone and upper layers II-IV of the cerebral cortex. J Comp Neurol. 479:168–180.
Nieto MA. 2001. The early steps of neural crest development. Mech Dev. 105:27–35.
Nieto MA. 2002. The snail superfamily of zinc-finger transcription factors. Nat Rev Mol Cell Biol. 3:155–166.
Nieto MA, Sargent MG, Wilkinson DG, Cooke J. 1994. Control of cell behavior during vertebrate development by Slug, a zinc finger gene. Science. 264:835–839.
Noctor SC, Martinez-Cerdeno V, Ivic L, Kriegstein AR. 2004. Cortical neurons arise in symmetric and asymmetric division zones and migrate through specific phases. Nat Neurosci. 7:136–144.
Nowakowski RS, Caviness VS Jr, Takahashi T, Hayes NL. 2002. Population dynamics during cell proliferation and neuronogenesis in the developing murine neocortex. Results Probl Cell Differ. 39:1–25.
Ohtsuka T, Sakamoto M, Guillemot F, Kageyama R. 2001. Roles of the basic helix-loop-helix genes Hes1 and Hes5 in expansion of neural stem cells of the developing brain. J Biol Chem. 276:30467–30474.
O'Leary DD, Sahara S. 2008. Genetic regulation of arealization of the neocortex. Curr Opin Neurobiol. 18:90–100.
Pacary E, Heng J, Azzarelli R, Riou P, Castro D, Lebel-Potter M, Parras C, Bell DM, Ridley AJ, Parsons M et al. 2011. Proneural transcription factors regulate different steps of cortical neuron migration through Rnd-mediated inhibition of RhoA signaling. Neuron. 69:1069–1084.
Peinado H, Del Carmen Iglesias-de la Cruz M, Olmeda D, Csiszar K, Fong KS, Vega S, Nieto MA, Cano A, Portillo F. 2005. A molecular role for lysyl oxidase-like 2 enzyme in snail regulation and tumor progression. EMBO J. 24:3446–3458.
Perron M, Furrer MP, Wegnez M, Theodore L. 1999. Xenopus elav-like genes are differentially expressed during neurogenesis. Mech Dev. 84:139–142.
Pontious A, Kowalczyk T, Englund C, Hevner RF. 2008. Role of intermediate progenitor cells in cerebral cortex development. Dev Neurosci. 30:24–32.
Rakic P. 2003. Developmental and evolutionary adaptations of cortical radial glia. Cereb Cortex. 13:541–549.
Rakic P. 2009. Evolution of the neocortex: a perspective from developmental biology. Nat Rev Neurosci. 10:724–735.
Rakic P. 1972. Mode of cell migration to the superficial layers of fetal monkey neocortex. J Comp Neurol. 145:61–83.
Rakic P. 1974. Neurons in rhesus monkey visual cortex: systematic relation between time of origin and eventual disposition. Science. 183:425–427.
Rakic P. 1988. Specification of cerebral cortical areas. Science. 241:170–176.
Rash BG, Grove EA. 2006. Area and layer patterning in the developing cerebral cortex. Curr Opin Neurobiol. 16:25–34.
Roark M, Sturtevant MA, Emery J, Vaessin H, Grell E, Bier E. 1995. Scratch, a pan-neural gene encoding a zinc finger protein related to snail, promotes neuronal development. Genes Dev. 9:2384–2398.
Rubenstein A, Merriam J, Klymkowsky MW. 1997. Localizing the adhesive and signaling functions of plakoglobin. Dev Genet. 20:91–102.
Sasaki S, Tabata H, Tachikawa K, Nakajima K. 2008. The cortical subventricular zone-specific molecule Svet1 is part of the nuclear RNA coded by the putative netrin receptor gene Unc5d and is expressed in multipolar migrating cells. Mol Cell Neurosci. 38:474–483.
Scardigli R, Baumer N, Gruss P, Guillemot F, Le Roux I. 2003. Direct and concentration-dependent regulation of the proneural gene Neurogenin2 by Pax6. Development. 130:3269–3281.
Scardigli R, Schuurmans C, Gradwohl G, Guillemot F. 2001. Crossregulation between Neurogenin2 and pathways specifying neuronal identity in the spinal cord. Neuron. 31:203–217.
Schuurmans C, Armant O, Nieto M, Stenman JM, Britz O, Klenin N, Brown C, Langevin LM, Seibt J, Tang H et al. 2004. Sequential phases of cortical specification involve Neurogenin-dependent and -independent pathways. EMBO J. 23:2892–2902.
Schwab MH, Druffel-Augustin S, Gass P, Jung M, Klugmann M, Bartholomae A, Rossner MJ, Nave KA. 1998. Neuronal basic helix-loop-helix proteins (NEX, neuroD, NDRF): spatiotemporal expression and targeted disruption of the NEX gene in transgenic mice. J Neurosci. 18:1408–1418.
Sekine K, Honda T, Kawauchi T, Kubo K, Nakajima K. 2011. The outermost region of the developing cortical plate is crucial for both the switch of the radial migration mode and the Dab1-dependent "inside-out" lamination in the neocortex. J Neurosci. 31: 9426–9439.
Seo S, Lim JW, Yellajoshyula D, Chang LW, Kroll KL. 2007. Neurogenin and NeuroD direct transcriptional targets and their regulatory enhancers. EMBO J. 26:5093–5108.
Sessa A, Mao CA, Hadjantonakis AK, Klein WH, Broccoli V. 2008. Tbr2 directs conversion of radial glia into basal precursors and guides neuronal amplification by indirect neurogenesis in the developing neocortex. Neuron. 60:56–69.
Seugnet L, Simpson P, Haenlin M. 1997. Transcriptional regulation of Notch and Delta: requirement for neuroblast segregation in Drosophila. Development. 124:2015–2025.
Shen Q, Zhong W, Jan YN, Temple S. 2002. Asymmetric Numb distribution is critical for asymmetric cell division of mouse cerebral cortical stem cells and neuroblasts. Development. 129: 4843–4853.
Shields JM, Christy RJ, Yang VW. 1996. Identification and characterization of a gene encoding a gut enriched *Krüppel*-like factor expressed during growth arrest. J Biol Chem. 271:20009–20017.
Smart IH, Dehay C, Giroud P, Berland M, Kennedy H. 2002. Unique morphological features of the proliferative zones and postmitotic compartments of the neural epithelium giving rise to striate and extrastriate cortex in the monkey. Cereb Cortex. 12:37–53.
Stoykova A, Treichel D, Hallonet M, Gruss P. 2000. Pax6 modulates the dorsoventral patterning of the mammalian telencephalon. J Neurosci. 20:8042–8050.
Sur M, Rubenstein JL. 2005. Patterning and plasticity of the cerebral cortex. Science. 310:805–810.
Tabata H, Nakajima K. 2001. Efficient in utero gene transfer system to the developing mouse brain using electroporation: visualization of neuronal migration in the developing cortex. Neurosci. 103:865–872.
Tabata H, Nakajima K. 2003. Multipolar migration: the third mode of radial neuronal migration in the developing cerebral cortex. J Neurosci. 23:9996–10001.
Tarabykin V, Stoykova A, Usman N, Gruss P. 2001. Cortical upper layer neurons derive from the subventricular zone as indicated by Svet1 gene expression. Development. 128:1983–1993.
Wu SX, Goebbels S, Nakamura K, Kometani K, Minato N, Kaneko T, Nave KA, Tamamaki N. 2005. Pyramidal neurons of upper cortical layers generated by NEX-positive progenitor cells in the subventricular zone. Proc Natl Acad Sci USA. 102:17172–17177.
Yamasaki H, Sekimoto T, Ohkubo T, Douchi T, Nagata Y, Ozawa M, Yoneda Y. 2005. Zinc finger domain of Snail functions as a nuclear localization signal for importin beta-mediated nuclear import pathway. Genes Cells. 10:455–464.
Zhang K, Rodriguez-Aznar E, Yabuta N, Owen RJ, Mingot JM, Nojima H, Nieto MA, Longmore GD. 2012. Lats2 kinase potentiates Snail1 activity by promoting nuclear retention upon phosphorylation. EMBO J. 31:29–43.
Zimmer C, Tiveron MC, Bodmer R, Cremer H. 2004. Dynamics of Cux2 expression suggests that an early pool of SVZ precursors is fated to become upper cortical layer neurons. Cereb Cortex. 14:1408–1420.